

Hydraulics Research
Wallingford

COMBINED NEAR AND FAR FIELD
MODELLING OF BUOYANT PLUMES

A J Cooper PhD

Report No. SR 144
January 1988

Registered Office: Hydraulics Research Limited,
Wallingford, Oxfordshire OX10 8BA.
Telephone: 0491 35381 Telex: 848552

This report describes work funded by the Department of the Environment under Research Contract PECD 7/6/61, for which the DoE nominated officer was Dr R P Thorogood. It is published on behalf of the Department of the Environment but any opinions expressed in this report are not necessarily those of the funding Department. The work was carried out by Dr A J Cooper in the Tidal Engineering Department of Hydraulics Research, Wallingford, under the management of Mr M F C Thorn.

C Crown Copyright 1987

Published by permission of the Controller of Her Majesty's Stationery Office.

ABSTRACT

Techniques for the numerical modelling of both the near field of a buoyant plume and the far field (long term build up) are available and are frequently used. In this report buoyancy is generally supposed to be due to temperature differences but the results are also applicable to other kinds of buoyant plume. In engineering applications it is usually the total field that is of interest. The results of the two model studies can be added together to give the total field only by an artificial technique to ensure that no effluent is counted twice.

The present report describes how the whole field may be modelled in such a way that the component fields may be added together correctly to yield the total field. This technique has been applied to the Hinkley Point power station thermal plume where near and far field model studies have previously been carried out separately and where a database of field observations exists. The heat reaching the open east and west boundaries of the 40m grid near field model was depth integrated and stored. This heat was then input to the appropriate cells of the 500m grid far field model, summing over all the 40m cells in each 500m cell. In this way the far field model computes the true background within the area of the near field model but the total heat field outside the near field model. This technique is equivalent to using a dynamically linked 3D-2D model. The combined power station heat field is worked out and compared with the field data.

The problem of plume bifurcation in the near field is also addressed. A literature review suggests that for cooling water plumes the bifurcation is due mainly to buoyancy driven secondary flow. Numerical model results demonstrate the phenomenon of plume bifurcation. Between the branches of the plume vertical upwelling occurs supplying ambient water. Downwelling occurs at the edges of the plume. In order to model plume bifurcation in a 3-D model it is necessary to have a sufficiently fine grid both in the horizontal and vertical directions to be able to resolve the secondary flow.

Sensitivity tests are reported which show how dependent the near field results are in the 3D model to the transport algorithm used. It is found that a flux corrected transport algorithm in which both spurious minima and maxima are prevented is the best scheme tested.

This report is the last of three reports on the mathematical modelling of buoyant plumes, the two previous reports being concerned with the effects of wind-induced mixing on buoyant plumes and with the validation of the HEATFLOW-3D model by comparison with data for the Hinkley Point plume. The techniques developed are a very powerful new tool for simulating buoyant plumes.

CONTENTS

	Page
1 INTRODUCTION	1
2 NEAR FIELD MODELLING	3
2.1 3D model transport algorithm	5
2.2 Plume bifurcation	6
2.3 Near field modelling of Hinkley Point	7
3 FAR FIELD MODELLING	8
3.1 Sensitivity tests	8
3.2 Far field modelling of Hinkley Point	9
4 COMBINED NEAR AND FAR FIELD MODEL	9
5 CONCLUSIONS	12
6 ACKNOWLEDGEMENTS	13
7 REFERENCES	14

FIGURES

1	Location map
2	Near field plume
3-5	Effect of flux-corrected transport
6	Bifurcated plume
7	Bifurcated plume schematic
8	Simulated plume isotherms peak ebb
9	Simulated velocity vectors ebb tide
10	Bifurcated plume cross sections
11	Vertical velocities in bifurcated plume
12	Heat output from near field model
13	Far field temperature distribution
14-19	Far field model sensitivity
20	Hinkley survey positions
21	True far field temperature histories
22	True far field temperature contours
23	Far field temperatures no primary heat
24	Total heat field - comparison with data

1 INTRODUCTION

Both near and far field studies of buoyant plumes have been carried out for many years. In order to give greater confidence in engineering predictions it is important to be able to obtain the total field including both the near and far field components.

The present work reviews techniques for joining together the near and far field. One such technique is described in detail and applied to the plume from Hinkley Point power station (Figure 1).

The buoyant plume caused by e.g. a cooling water discharge may be divided into the near and far fields. The distinction between these fields must be artificial as in nature the same physical processes operate on all space and time scales. Nevertheless a conceptual separation can be carried out based on the dominant physical processes in different areas.

Near to the outfall the appearance of the heat field is of a surface jet-like structure or a plume rising from the bed to the surface. This contains water which has been recently discharged (within a few hours at most) and diluted by ambient water. However, the ultimate fate of the discharged heat is to be exchanged with the atmosphere and this requires a very large area of sea to have its surface temperature raised. This takes a long time (several days at least) to come to an equilibrium and is not greatly dependent on the details of the outfall.

It therefore seems that a simple decomposition into a near field plume (dominated by momentum and buoyancy) and a background field (dominated by ambient advection, diffusion and heat loss and unaffected by buoyancy and momentum) should be possible. This is the origin of the idea of near and far field models.

Far from the outfall the far field model can give a good representation of the heat field in the region where the temperature excess above the ambient is small. Near to the outfall, however, it is unclear what meaning should be attached to the far field temperature.

It is certainly true that the continuous discharge of hot water for a long period raises the background (ambient) temperature in the vicinity of the outfall. Thus knowing the background temperature there one can add it to the near field plume temperature to obtain the complete heat field near to the outfall. However, it is clear that this background heat field is due only to that heat which was discharged several hours or several days previously and the more recently discharged heat forms the near field plume.

So it seems necessary to run the far field model with no heat input during a period of a few hours or days previous to the time at which the background temperature rise at the outfall is needed, in order not to count heat twice when the near field is added.

A further complication is that the background heat field near to the outfall does depend on the assumed position of heat input to the far field model. In reality it depends on the process whereby the plume water is moved by the tidal current and diluted by turbulence. Therefore it is necessary to approximate this process and estimate where the heat is input, although the heat field is unlikely to be very sensitive to where this is (see Section 3.1).

Given the concept of the decomposition of the physical heat field into the plume and the background temperature it is now possible to describe the models used (Sections 2 and 3) Section 2 includes a

discussion of the possibility of simulating near field plume bifurcation. Section 4 is a description of the combined near and far field model.

2 NEAR FIELD MODELLING

Plume modelling in the near field is achieved primarily using one of the following techniques:

- 1 Integral jet model
- 2 Diffusion plume model
- 3 Random walk model
- 4 3D plume model

In any case the model is run for a small number of tides to give a repeating near field plume. After some time or beyond a certain distance the plume shades off into the background field. The background can be taken to be vertically well mixed.

An integral jet model is suitable for discharges at the surface which have momentum. It is usually run as a steady state simulation (suitable for example for lake discharges). The driving force for plume mixing is taken to be the differential movement of plume and ambient. An unsteady version of this model has also been developed for jet discharges into tidal waters (Ref 3). The jet takes the discharged effluent offshore where it forms a background field. This kind of model ignores the presence of a coast or sea bed so the effects of isotherm attachment to the coast or plume attachment to the bed are not included.

The diffusion and random walk plume models have similar functions. Their main application is for effluent discharges from the bed into tidal currents. The effluent is advected with the current but diffuses

across it. The turbulent diffusion is represented either by assuming a diffusion law and Gaussian profiles or by having an ensemble of particles each of which executes random steps. The plume is initially on the surface at the outfall but after less than about a tide in coastal waters the plume will be well mixed through the depth and will form a background field. The relative advantages of diffusion and random walk models depend mainly on economics.

The three dimensional numerical flow model for buoyant plumes is a fairly new innovation and is applicable mainly to large effluent discharges (such as river plumes and power station thermal discharges). The model can realistically include the presence of the sea bed, coast etc. As the 3D model includes all of the important physical process it should be able, in principle, to simulate both the near and far fields. However 3D models are expensive in computer time and the need to run the far field for many tides to obtain the background field would make excessive demands on present 3D models, except for small enclosed systems eg lakes . Another difficulty is that it would be hard both to resolve conditions near to the outfall and to extend the model far away in order to model the far field. The 3D model is often used to simulate a "mid field" plume (i.e. after the plume rise phase but before the far field). Because the Hinkley Point plume has been studied using a 3D model (Ref 1) and the far field has also been studied (Ref 2) and there is a lot of data available for this site (see e.g Figure 2) it was chosen for the present study.

2.1 3D model transport algorithm

Because of the strong horizontal concentration gradients which occur in the near field (see Figure 2)

it is often not satisfactory to use first order upstream differences for calculating the transport of pollutant as it involves a great deal of numerical diffusion. For this reason a flux correction step is often included in the calculation. This gives a "flux corrected transport" (fct) algorithm. The principle of this method is to compute the extra diffusion due to the upstream differencing and then to subtract it (i.e. to put in that amount of negative diffusion). However negative diffusion is notoriously unstable so a check is then made as to whether a new maximum and/or minimum value is introduced and at any such point the correction step is not made, or a smaller correction may be made.

In the past (Ref 1) the same version of this technique has been used in 3D near field modelling as is used in background temperature modelling i.e. to check for and eliminate only spurious minima but not spurious maxima (Ref 4). This prevents temperatures lower than the ambient value occurring which would be absurd. However in application to the near field this method was found in some cases to be giving temperatures greater than that of the water being discharged.

As this was not satisfactory the flux corrected transport algorithm used in the HEATFLOW-3D program was changed to eliminate both spurious minima and maxima, consequently it involves more diffusion than before. Results for the Hinkley Point power station plume using three schemes;

1. Upstream differencing
2. fct eliminating spurious minima
3. fct eliminating both spurious minima and maxima

are shown in Figures 3, 4 and 5. These figures show time histories of the temperature above ambient in the

top three layers of the model for a spring tide, all three layers are of depth 1m. Comparison with field data in the form of the temperature difference between surface and bed is also shown. It can be seen how scheme 2 tends to give excessively high peaks which are due to the fct formulation. Scheme 3 should be the best for most practical applications.

2.2 Plume bifurcation

Near field plume bifurcation is often found, particularly for thermal plumes, and is difficult to model numerically. This phenomenon is demonstrated in Figure 6 which shows the surface temperatures in a power station plume as observed in the infrared. The plume splits into two branches between which the water is near to the ambient temperature.

The explanation of plume bifurcation is that the plume buoyancy causes a secondary circulation with an outward surface flow and an inward flow beneath, with upwelling on the centreline (see Ref 5). This buoyancy-induced flow then advects the plume, pushing it outwards at the surface and upwards in the middle bringing in cold water. Finally the plume splits into two branches and ambient water occupies the space in between. This process is summarised in Figure 7. Another explanation in terms of vortices induced in the rising plume by the ambient current, which are then forced apart by the effect of the free surface (image vortex effect), as described in Ref 6 does not seem to be the dominant process for cooling water plumes discharging into shallow water.

One 3D numerical model simulation of a buoyant plume carried out at HR has produced such a bifurcated plume. Figure 8 shows the temperatures for the power station plume in four layers at a time during the ebb tide, the top three model layers are each 1m thick and

the remaining layer contains the rest of the water column. The temperature contours shown are of excess temperature above ambient. The corresponding velocity vectors in the four model layers are shown in Figure 9. This shows divergence in the area between the plume branches in the surface layer and convergence in the bottom two layers implying that vertically upwards flow is occurring. Convergence also occurs at the plume front where downwelling occurs. Figure 10 shows plume cross sections at the same time. The temperature contours shown in this figure are 1 to 6 degrees above ambient at 1 degree intervals. The plume bifurcation can be discerned in most of the cross sections.

Clearly if the preceding explanation is correct the numerical grid must be fine enough both in the vertical and horizontal directions to be able to resolve the secondary current system produced by buoyancy. Because the HEATFLOW-3D model is intended to represent buoyancy effects correctly, the model, with a fine enough grid, should be capable of correctly simulating the bifurcation.

An HR Report (Ref 8) is in preparation in which the physics of bifurcation is explored in more detail using survey observations the Fawley power station plume in the Solent.

2.3 Near field modelling of Hinkley Point

The use of the HEATFLOW-3D model to simulate the near field of the Hinkley Point power station plume and the validation of the model have been fully described in Ref 1. A 40m grid was used (see Figure 1). The model results were compared with aerial infra red imagery data and also with in situ thermistor data. Figure 2 shows a comparison of the

simulated surface temperatures at a particular time with observed surface temperatures. The near field for Hinkley is often called the mid field, the term near field then refers only to the flow down the outfall channel and across the rock platform.

3 FAR FIELD MODELLING

The far field is defined to be an area where the plume has become well mixed through the water column so that depth-integrated models are suitable for simulation. The background temperatures for Hinkley Point have been previously studied (Ref 2) and also compared with data (Figure 12).

The "true" far field in these studies has been found by omitting heat input during the last tide. This is necessary so that the near field can be added without the same heat being counted twice. This may be quite a doubtful procedure as it results in a non-continuous condition at high water (See Figure 16). The true far field would be continuous from one tide to the next.

As the heat is actually distributed to the far field by the near field plume it was thought worthwhile to carry out tests of sensitivity of the far field model temperatures to different ways of inputting heat.

3.1 Sensitivity tests

Figures 14 to 19 show the sensitivity of the far field temperatures for the Hinkley Point model for a mean tide to

1. Repeating heat field, constant heat input at the outfall location
2. Leaving out heat input during the last tide
3. Representing the outfall as heat input from the near field model at points A and B (see Figure 19)

In case 3 the heat input was at A during the ebb and B during the flood. The heat input in this case was taken to be a sinusoidal function of time whose time-average value was the same as in case 1. The phase was chosen so that the heat input was zero at high and low water and maximum at peak ebb and flood. This function was chosen because the heat is ponded in the area of the outfall near to slack water and does not enter the far field until later. The three cases were all computed for a mean tide. The results for case 2 show that the heat field obtained by leaving out the heat input for one tide is not continuous. The results for case 3 show that the far field heat distribution may be sensitive to how the heat is input.

3.2 Far field modelling of Hinkley Point

Far field modelling of Hinkley Point using the HEATFLOW-2D model has been described in Ref 2. A numerical model grid size of 500m in the vicinity of Hinkley Point was used. For this study the true background was computed by leaving out the heat input during the last tide, i.e. using method 2 above.

4 COMBINED NEAR AND FAR FIELD MODEL

Perhaps the most natural approach to combining the near and far fields would be to use one model for the whole field, but then it would have to contain all of the relevant physics and be able both to resolve small scale variations near the outfall and also to cover a large area to simulate the far field. Except for

small enclosed systems, such as lakes this is not presently practicable.

Another approach would be to have near and far field models with information passed between them. This is the approach taken here. If a 3D near field model and a 2D depth-integrated far field model are used then any effluent entering the far field model from the near field model will be mixed through the water column. The technique is therefore satisfactory unless heat returns to the area of interest still stratified. For the present study of Hinkley Point this is unlikely to be a problem because the tidal currents are large and the resulting turbulence tends to mix the returning heat through the depth.

For the study of Hinkley Point the heat reaching the east and west boundaries of the HEATFLOW-3D near field model was first depth integrated and then stored in a file so that it could be input at the corresponding positions in the 500m far field model. To do this all of the near field 40m cells which fall inside a particular 500m cell were summed to give the heat input to the 500m grid.

This technique results in the far field model simulating the true background within the limits of the near field model but elsewhere it gives the total field. The technique allows the near and far fields to be simply added together without heat being counted twice or not at all. In addition it involves little error because the heat lost from the near field model and then returning later will usually be well mixed through the depth by then.

The far field temperatures obtained by using the heat input from the near field model are shown in Figures 21 and 22. Comparing Figure 21 with Figure 23 (in

which heat input during the last tide is omitted) it can be seen that the simple omission of heat for the last tide gives a good representation except for the first and last 2-3 hours. The result with heat input omitted cannot be correct at those times because it is not continuous.

In Figure 21 the model gives the true background between frames 3 and 8 as the heat input occurs in frames 2 and 9. Further away the model predicts the total heat field.

The model has been set up so that it is possible simply to add together the near and far field heat within the near field model area to give the total power station heat field. Heat is conserved in this process as all heat lost from the near field is then present in the far field. Heat in the near field model area of the far field model is not transferred back to the near field model because its only effect there is to cause a rise in the ambient temperature.

The result of the addition is shown in Figure 24. This shows the bed temperatures (ie the far field) and surface (ie near plus far field) total power station heat fields a survey positions M and N (positions shown in Figure 20).

Comparison is also shown in this figure with the survey temperatures for two tides on 19.7.83 and 20.7.83 when the tidal range was about 6.5m. Because the temperature field at Hinkley is affected not only by the power station heat field but also by natural temperature variations which would also occur in the absence of a power station, the survey temperatures were corrected to give a estimate of the part of the temperature field due to the power station. This was achieved by subtracting the temperature variations due

to the estuarial temperature gradient. The variation this causes at each station was supposed to be sinusoidal with the peak at lower water and minimum at high water. The amplitude of the variation was estimated from the temperatures at the site and the 8km away the temperature values that result from this procedure may still include other natural heat variations (eg due to the solar heating of the water on Stert Flats) but these have been shown to be most significant during neap tides which read high water at or near noon (Ref 7). The tides under consideration do not satisfy this criterion and the inshore solar heat field was therefore assumed to be negligible. The process of obtaining the power station heat field is described in more detail in Ref 7.

The comparison of the model and observed surface and bed temperatures shown in Figure 24 shows that the features of the observations are simulated by the model to within the accuracy of repetition of the observed temperatures on successive tides.

5 CONCLUSIONS

The occurrence of near field plume bifurcation has been shown to result from buoyancy driven secondary flow. Downwelling occurs at the front between the plume and the ambient current and upwelling occurs behind causing ambient water temperatures between the two plume branches. Simulation of bifurcation in a 3D model therefore requires adequate resolution in both the vertical and horizontal directions.

It is also found that in near field studies it is better to use a flux corrected transport algorithm that removes spurious maxima and minima rather than the technique used in far field modelling where only spurious minima are prevented.

7 REFERENCES

1. Validation of a 3D numerical model of a buoyant plume. A J Cooper. Hydraulics Research Report No SR 121, March 1987.
2. Hinkley Point C Pre-application studies. Power station background temperature and siltation studies with and without the Severn Barrage. Report No EX 1254, Hydraulics Research Ltd 1985.
3. Cooper A J. Buoyant plume in an unsteady environment. 2nd International Symposium on Stratified Flows, Trondheim, 1980.
4. Miles G V. Numerical simulation of Sizewell background heat field, 10th AHR Congress, 1979, Vol 4, pp 347-354.
5. Rodi W and Weiss K. Experiments on coaxial heated water discharges. Journal of the Hydraulics Division ASCE volume 108, HY6, 1982.
6. Hayashi T. Turbulent buoyant jets of effluent discharged vertically upwards from an orifice in a cross-current in the ocean. IAHR 19th Congress, Paris, 1971.
7. Miles G V and Walmsley N. Validation of dispersion models submitted to Water Modelling and Measurement 2, Harrogate, 1988.
8. Spread of a surface thermal plume in coastal water. Report No SR 140, Hydraulics Research Ltd, 1988.

FIGURES

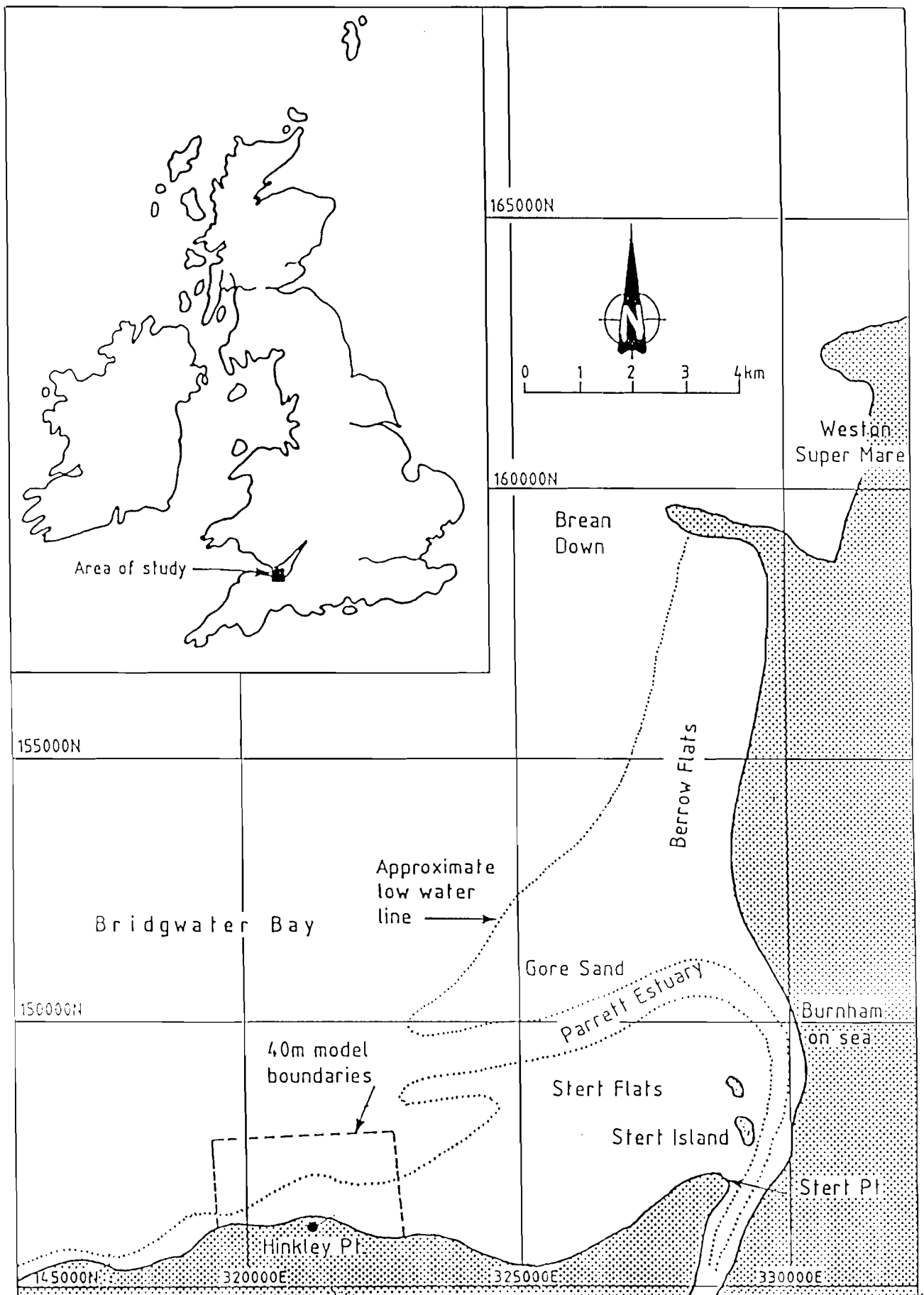
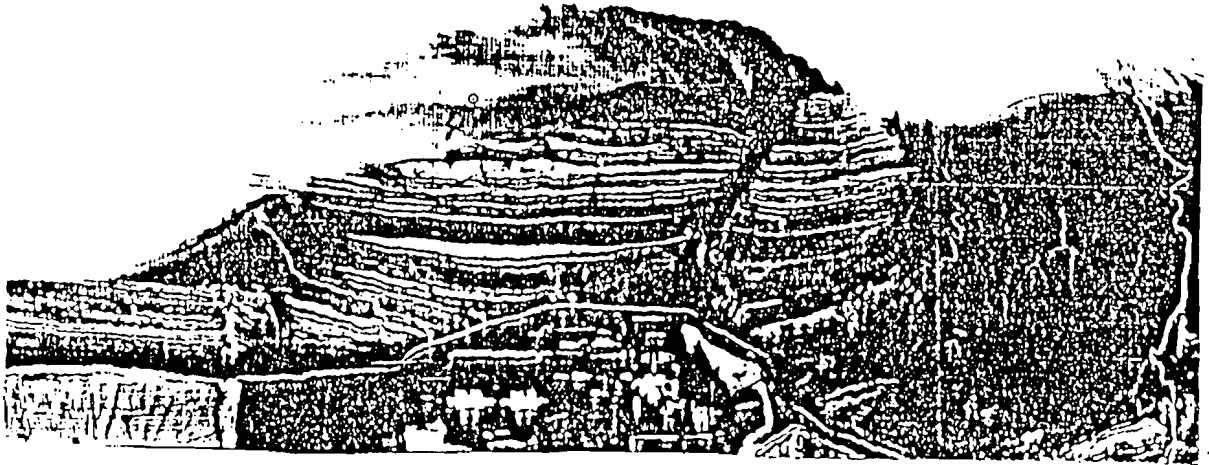


Fig 1 Location map

1 Observed

FLYING HEIGHT 3000 FT
RUN 6 TIME 13-10
14 MAY 1980



2 Simulated

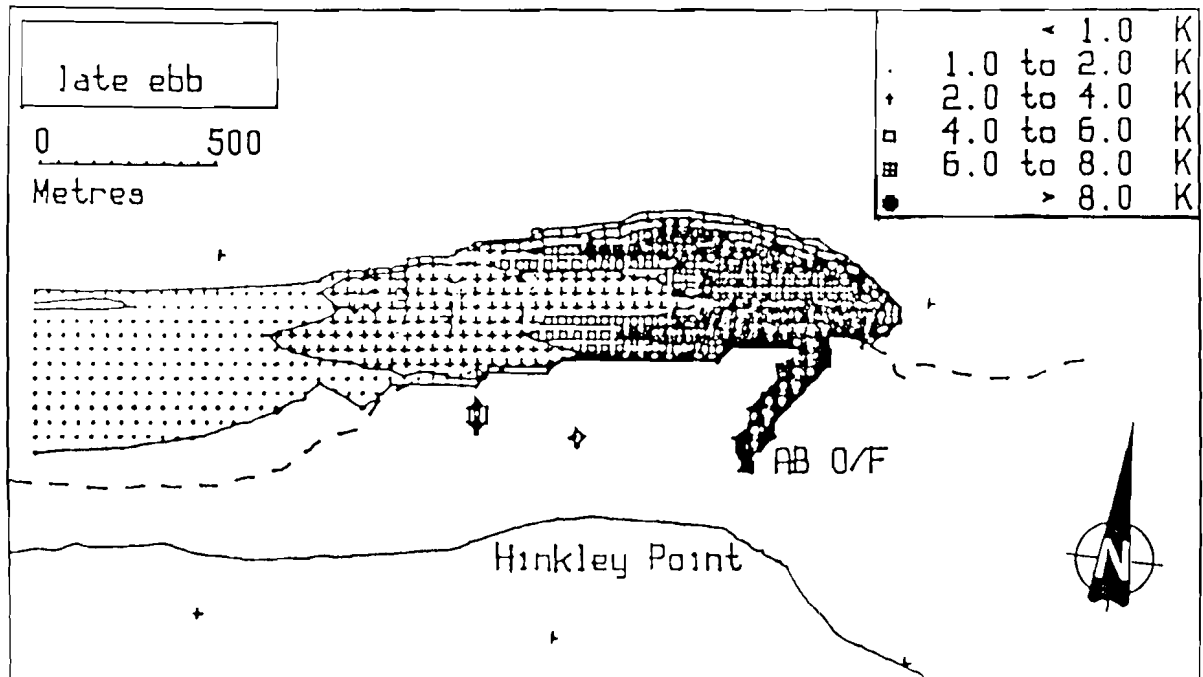


Fig 2 Near field plume

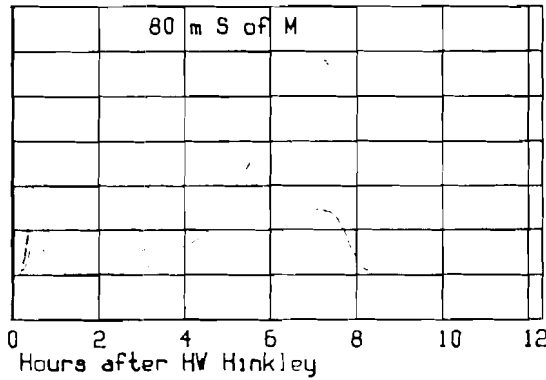
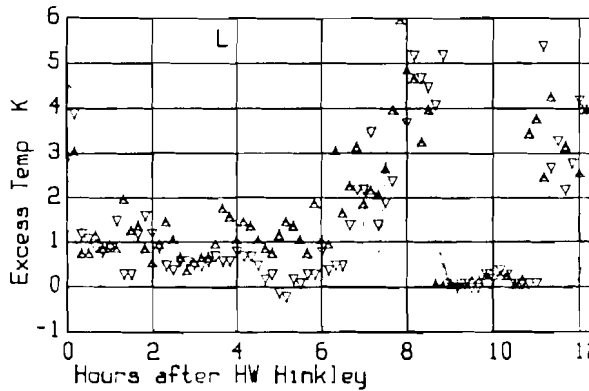
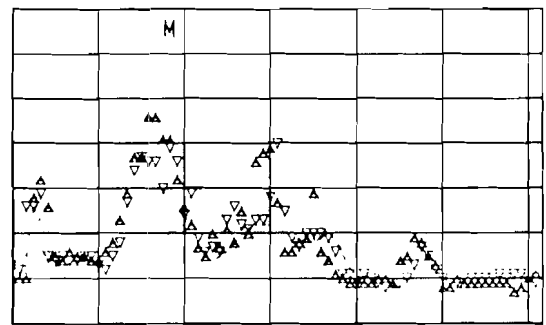
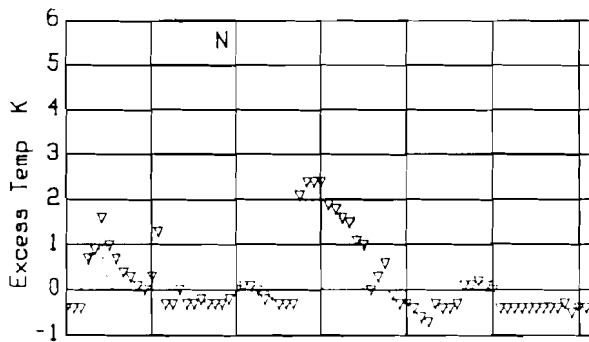
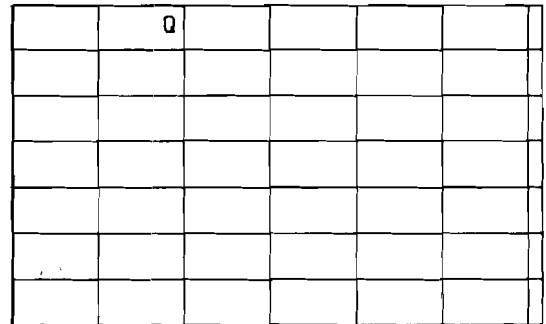
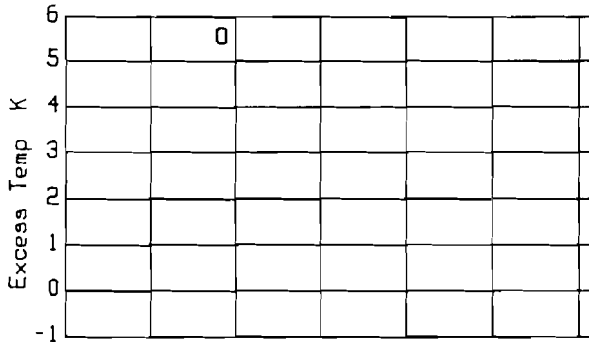
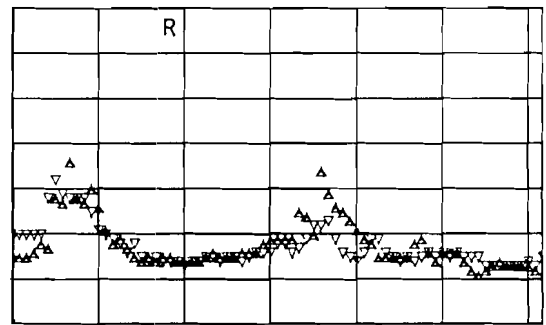
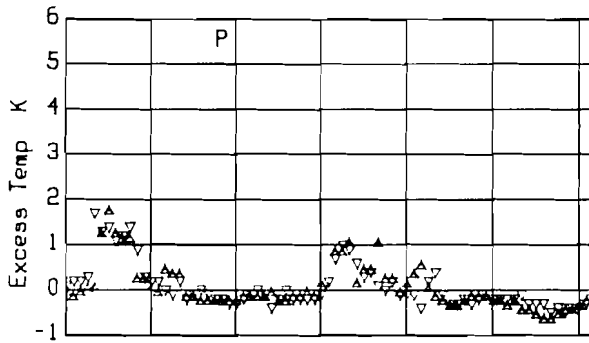
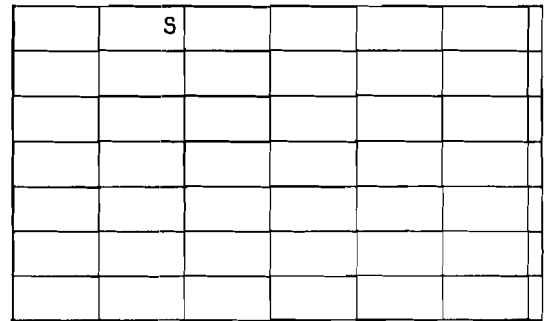
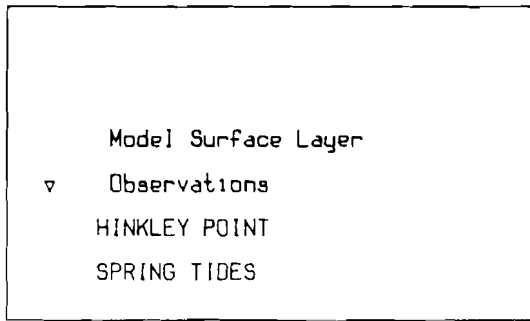


Fig 3 Effect of flux-corrected transport
Upstream differences

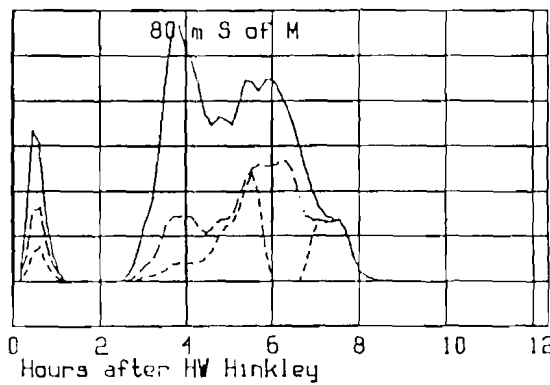
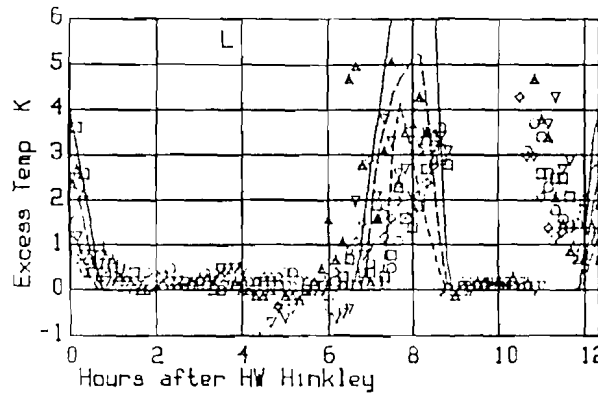
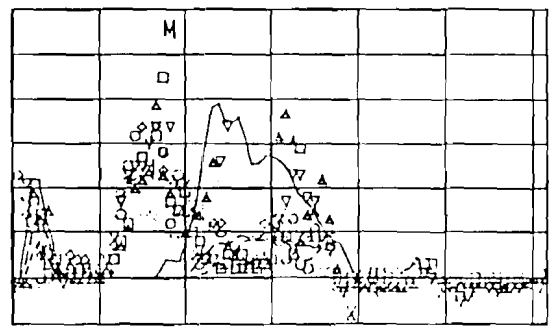
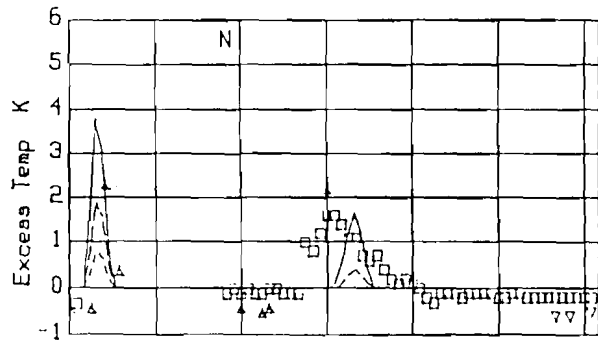
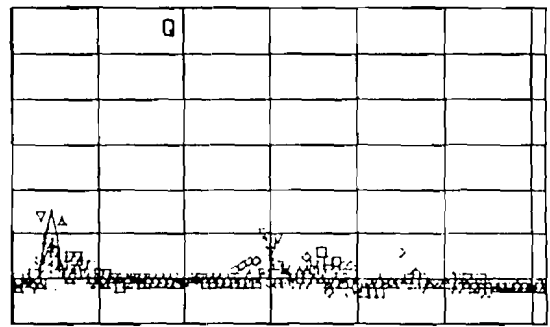
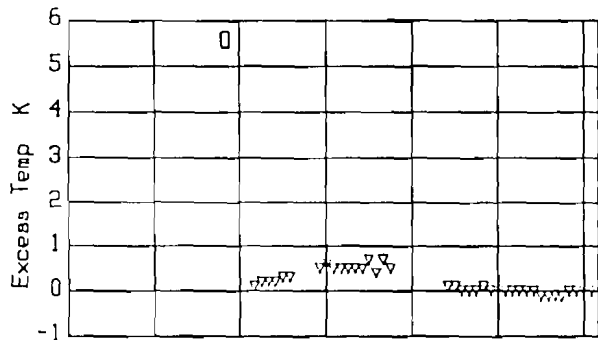
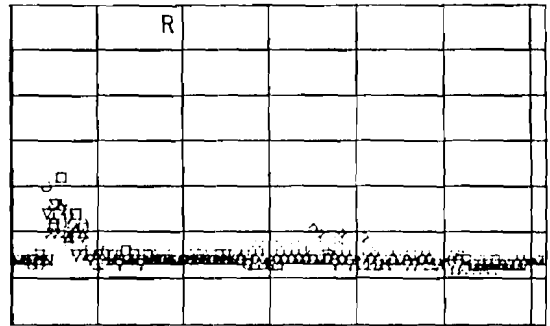
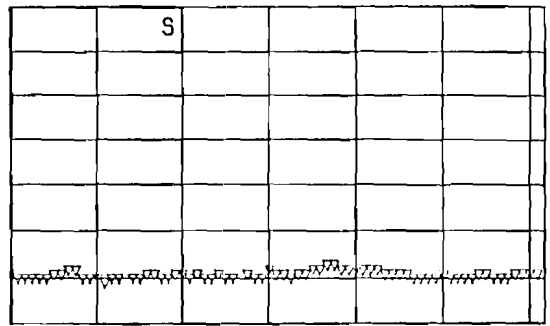
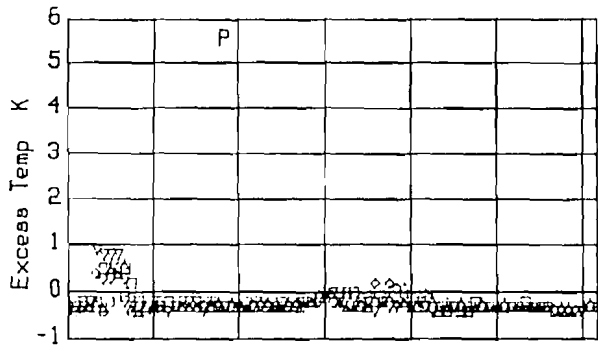
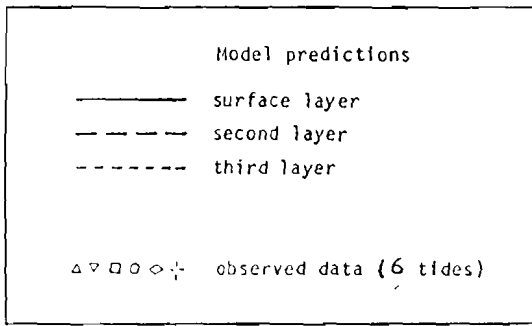


Fig 4 Effect of flux-connected transport
Removes minima

Model Surface Layer
 ▽ Observations
 HINKLEY POINT
 SPRING TIDES

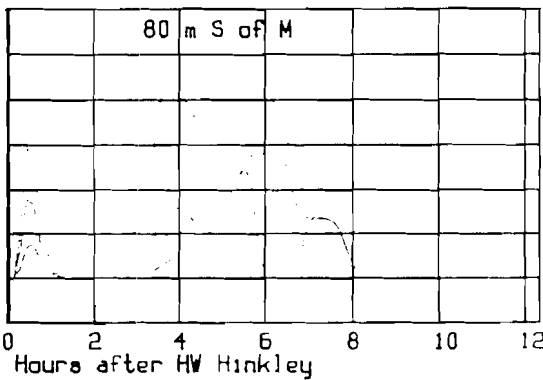
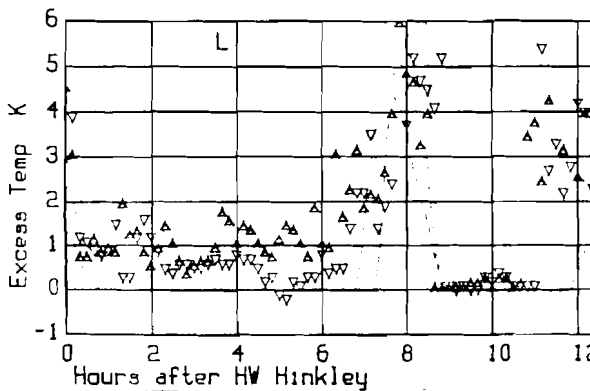
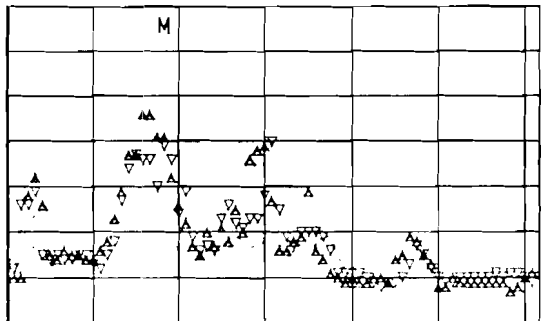
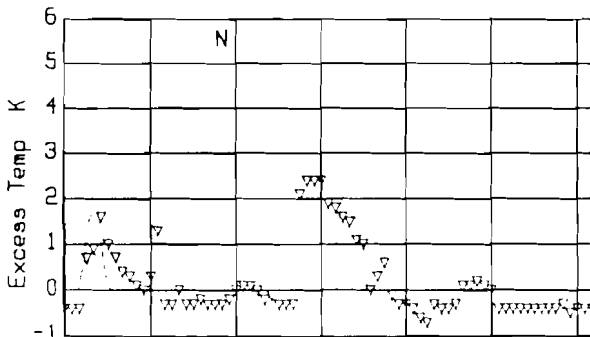
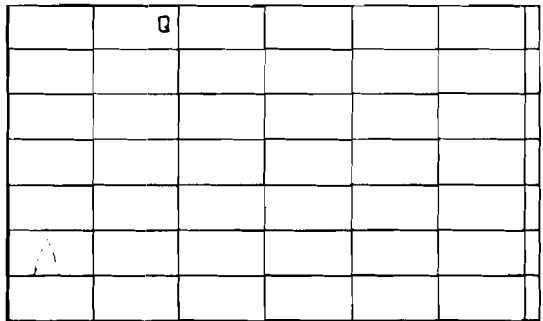
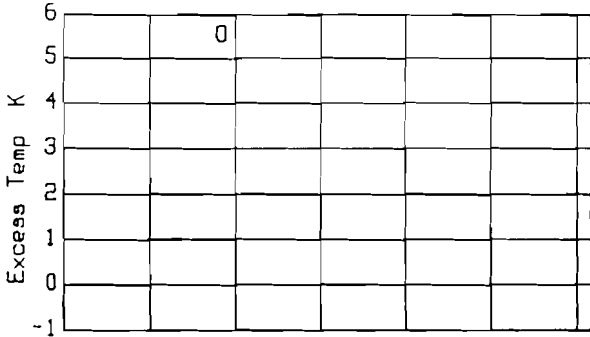
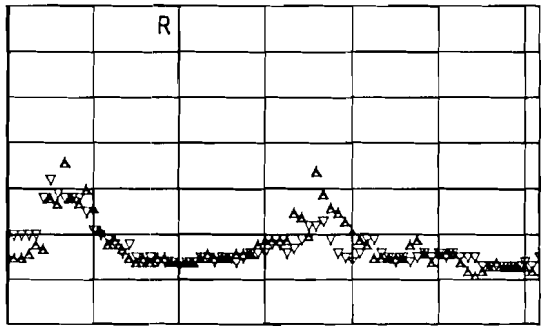
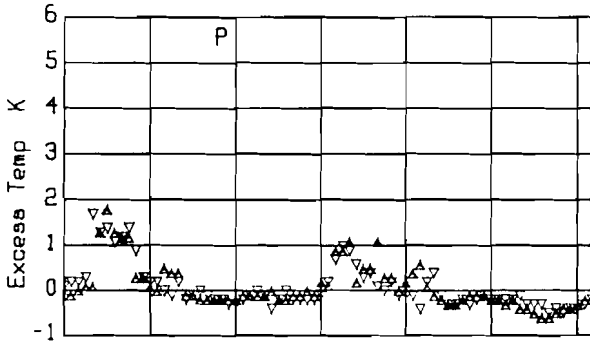
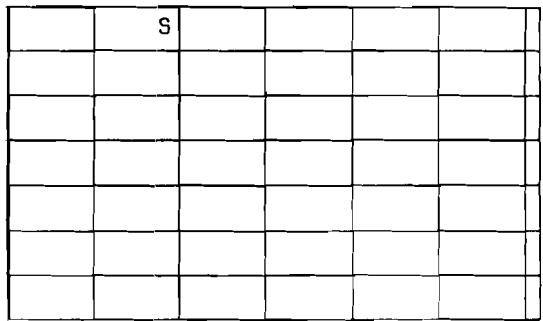


Fig 5 Effect of Flux-connected transport
 Removes minima & maxima

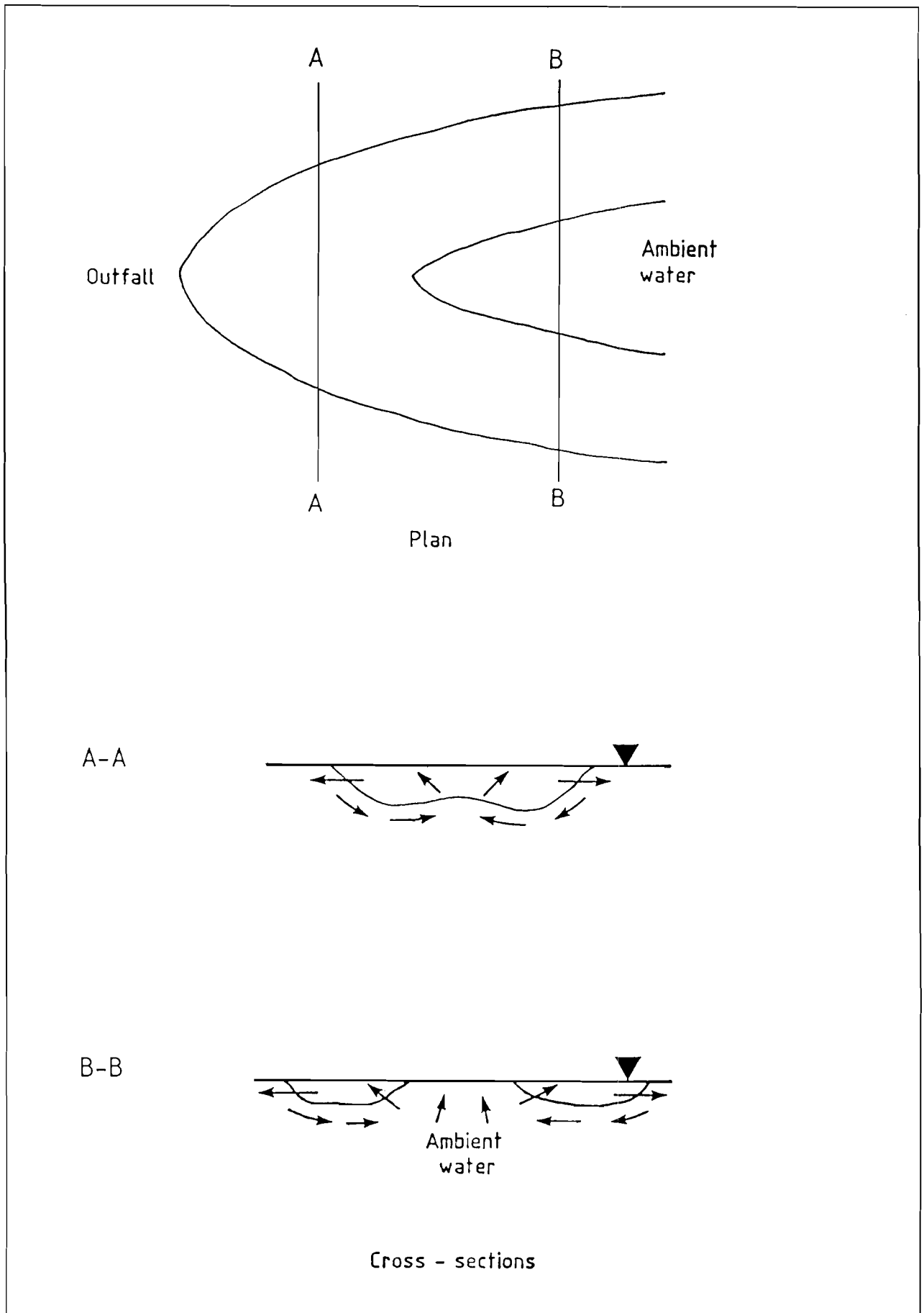


Fig 7 Bifurcated plume schematic

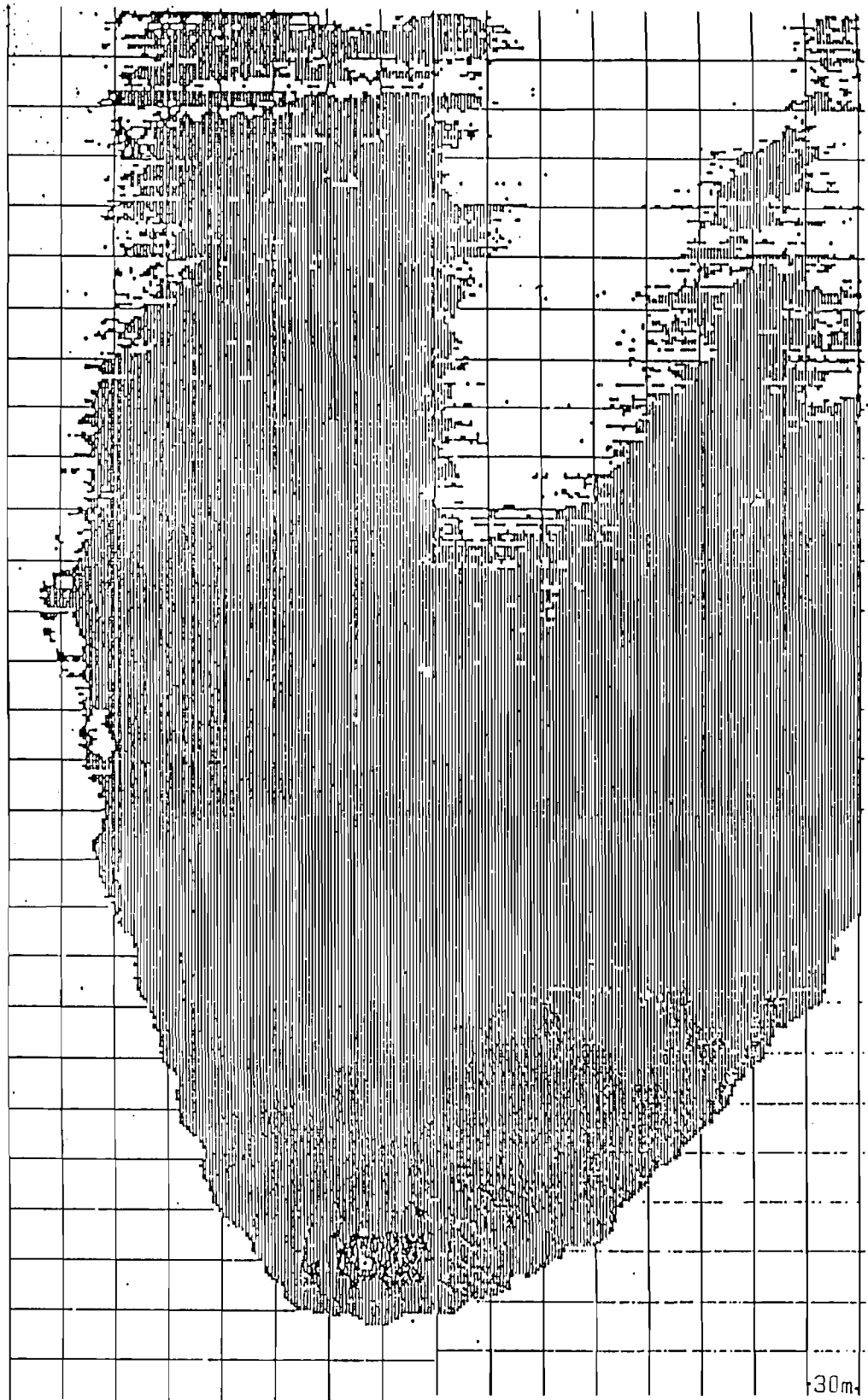


Fig 6 Bifurcated plume
After Fischer, List, Koh, Imberger and
Brooks 1979 -
Mixing in Inland and Coastal Waters

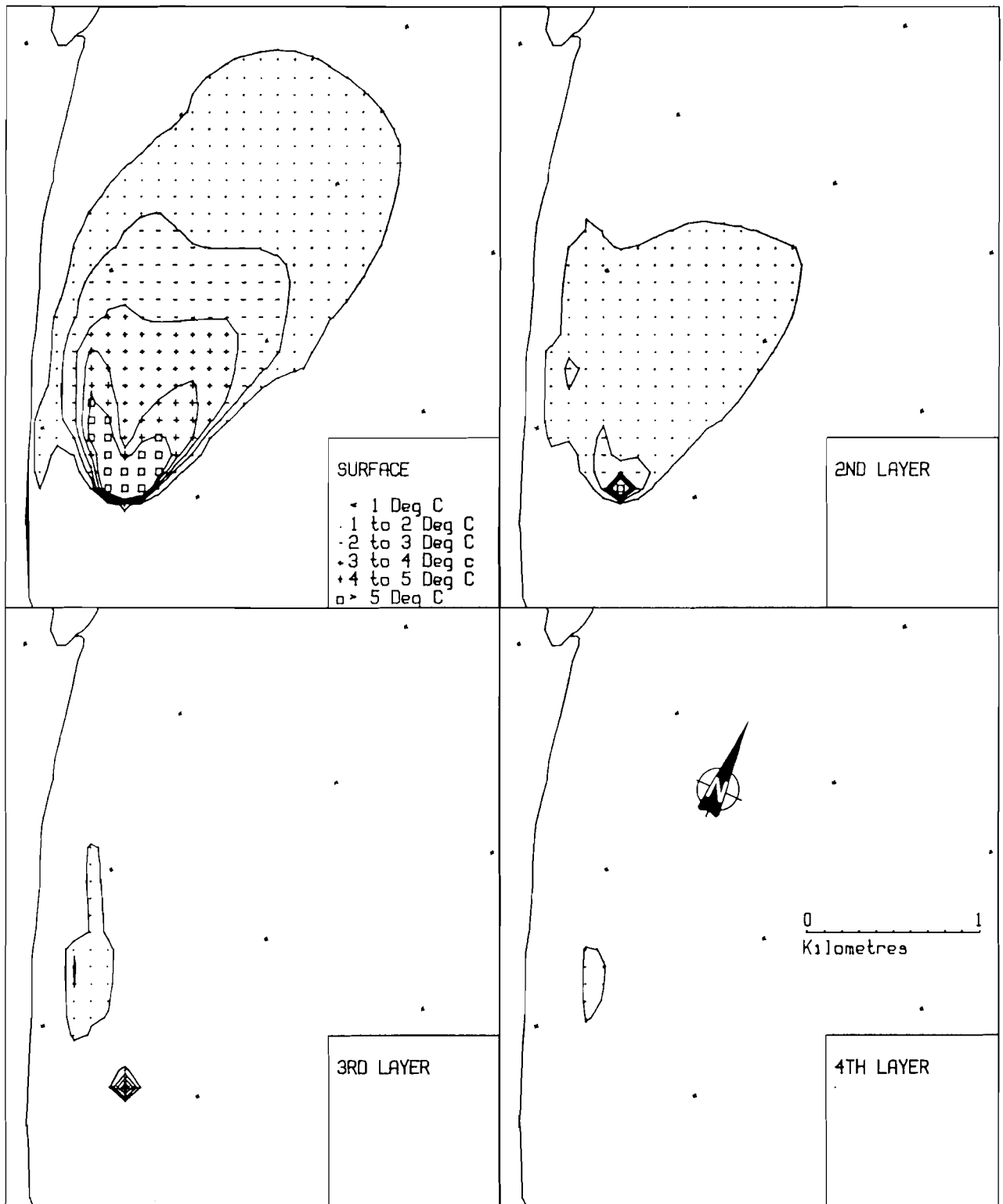


Fig 8 Simulated plume isotherms peak ebb

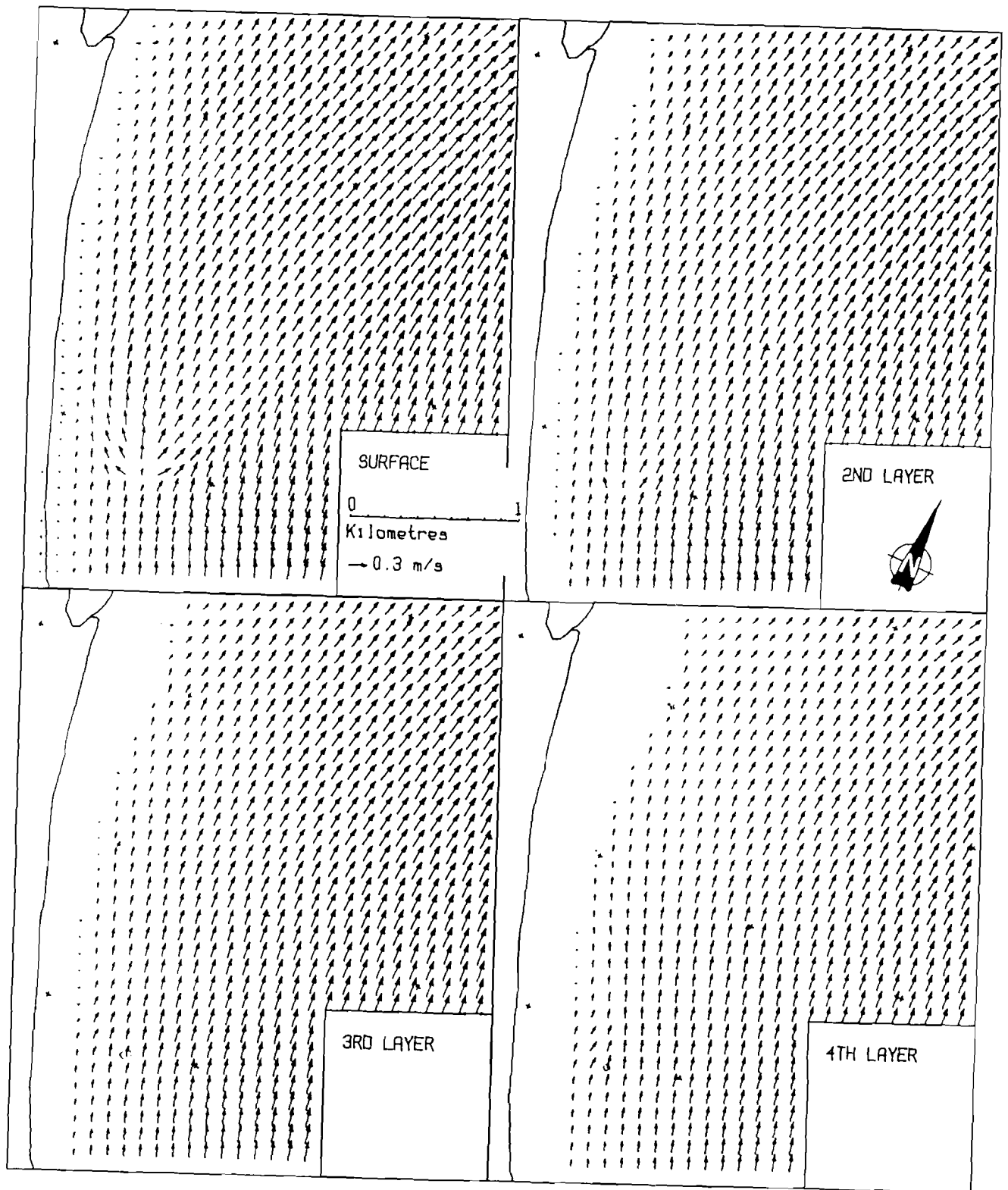


Fig 9 Simulated velocity vectors ebb tide

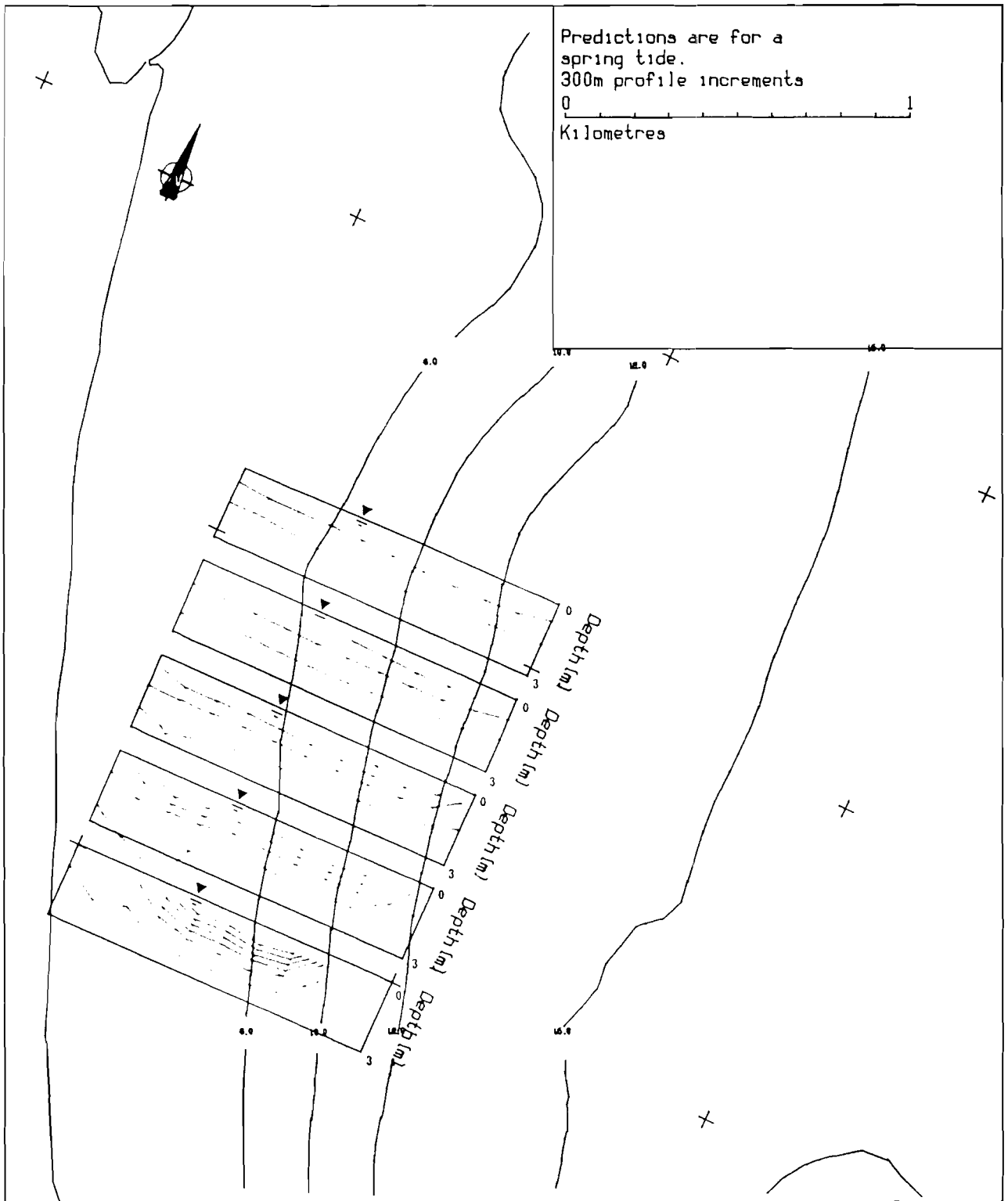


Fig 10 Bifurcated plume cross-sections

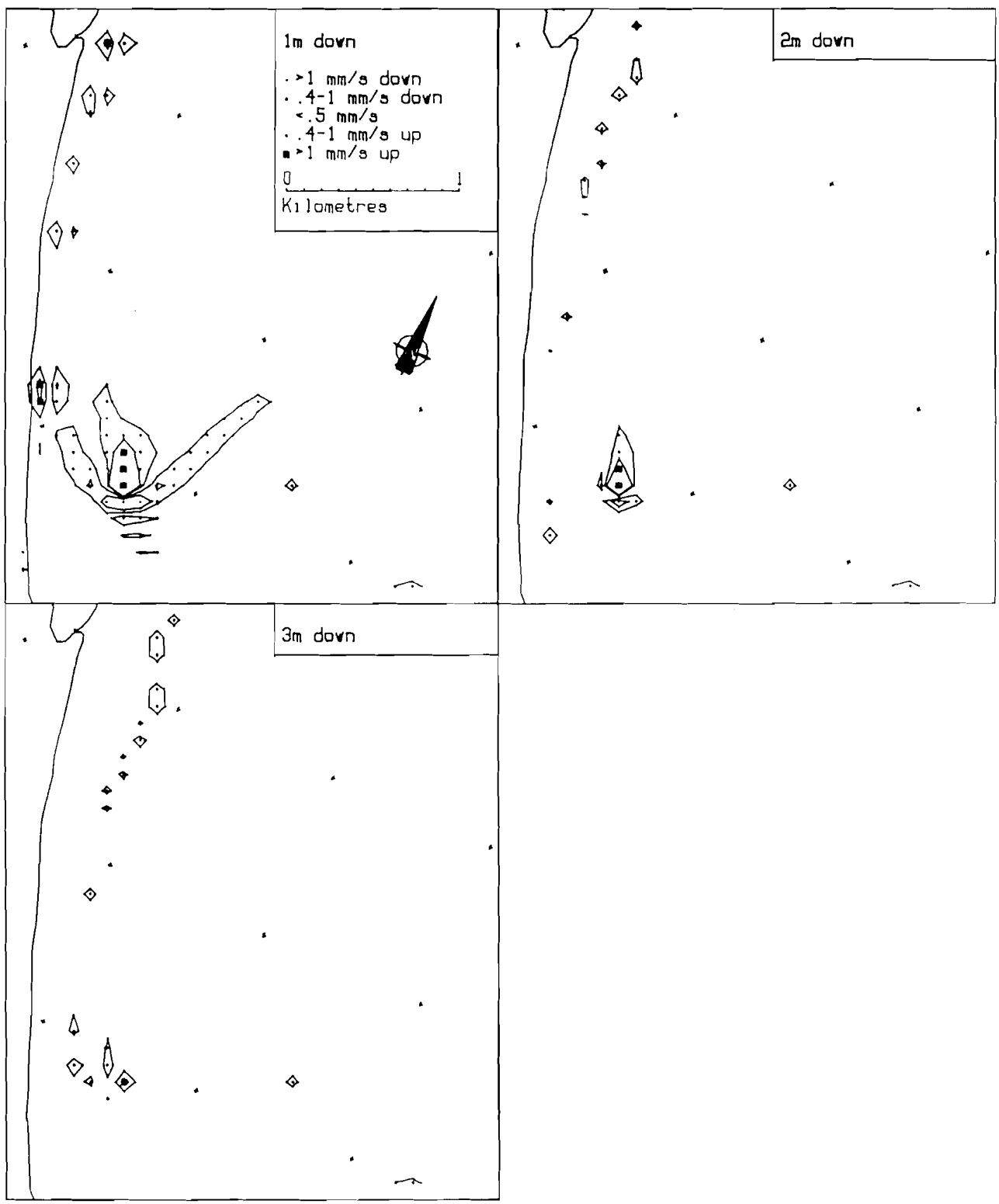


Fig 11 Vertical velocities
in bifurcated plume

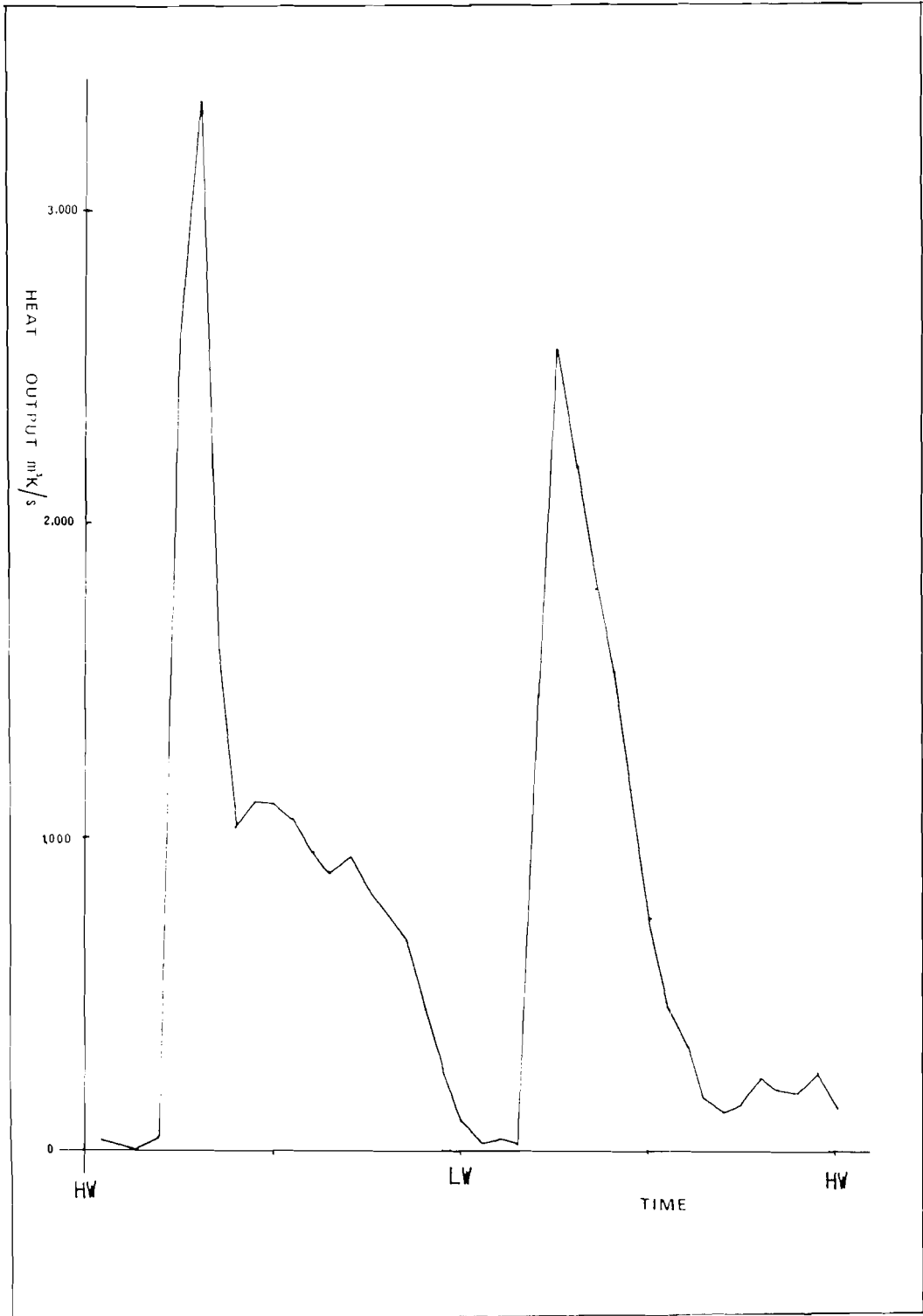


Fig 12 Heat output from near field model

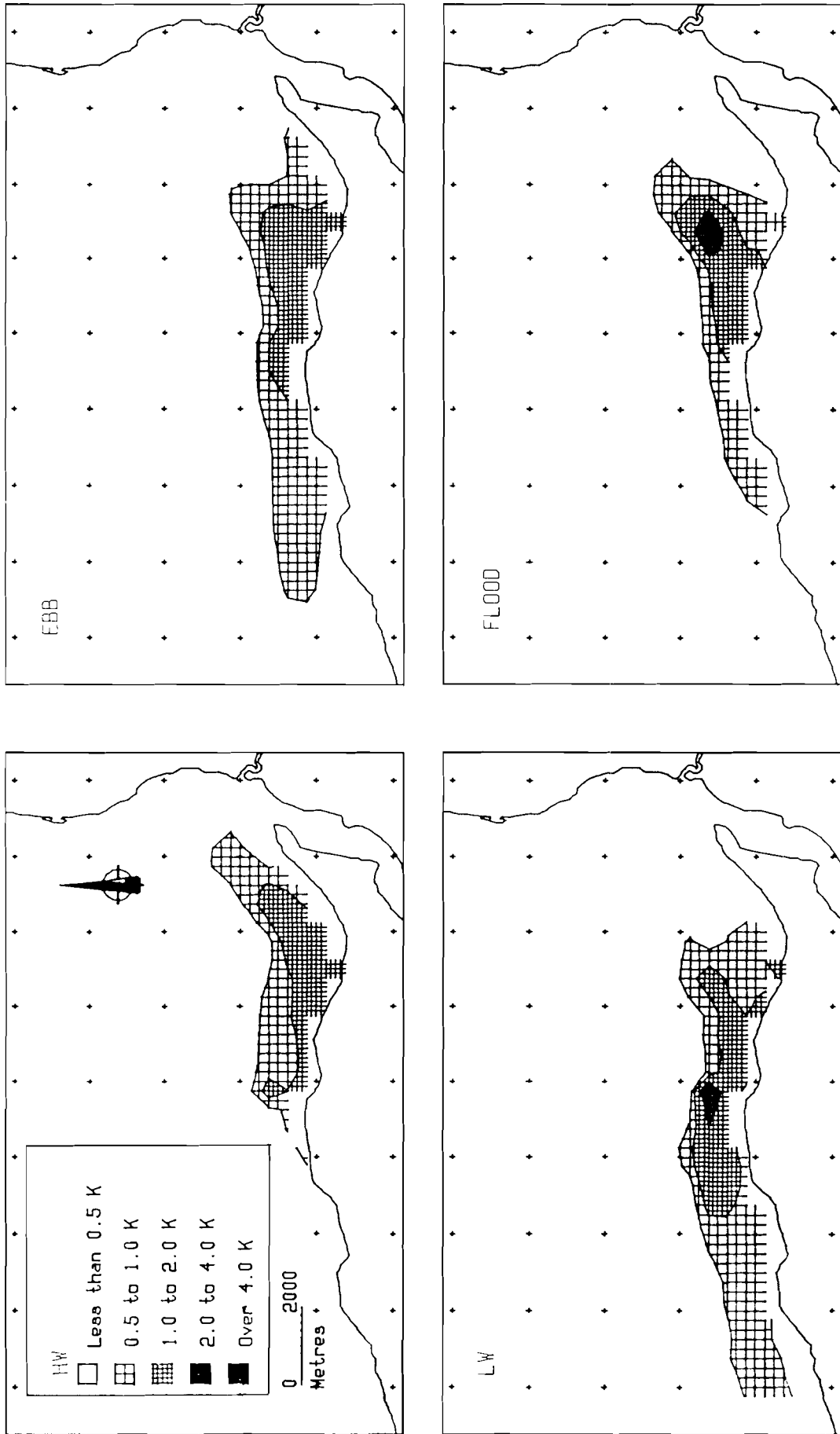


Fig 13 Far field temperature distribution

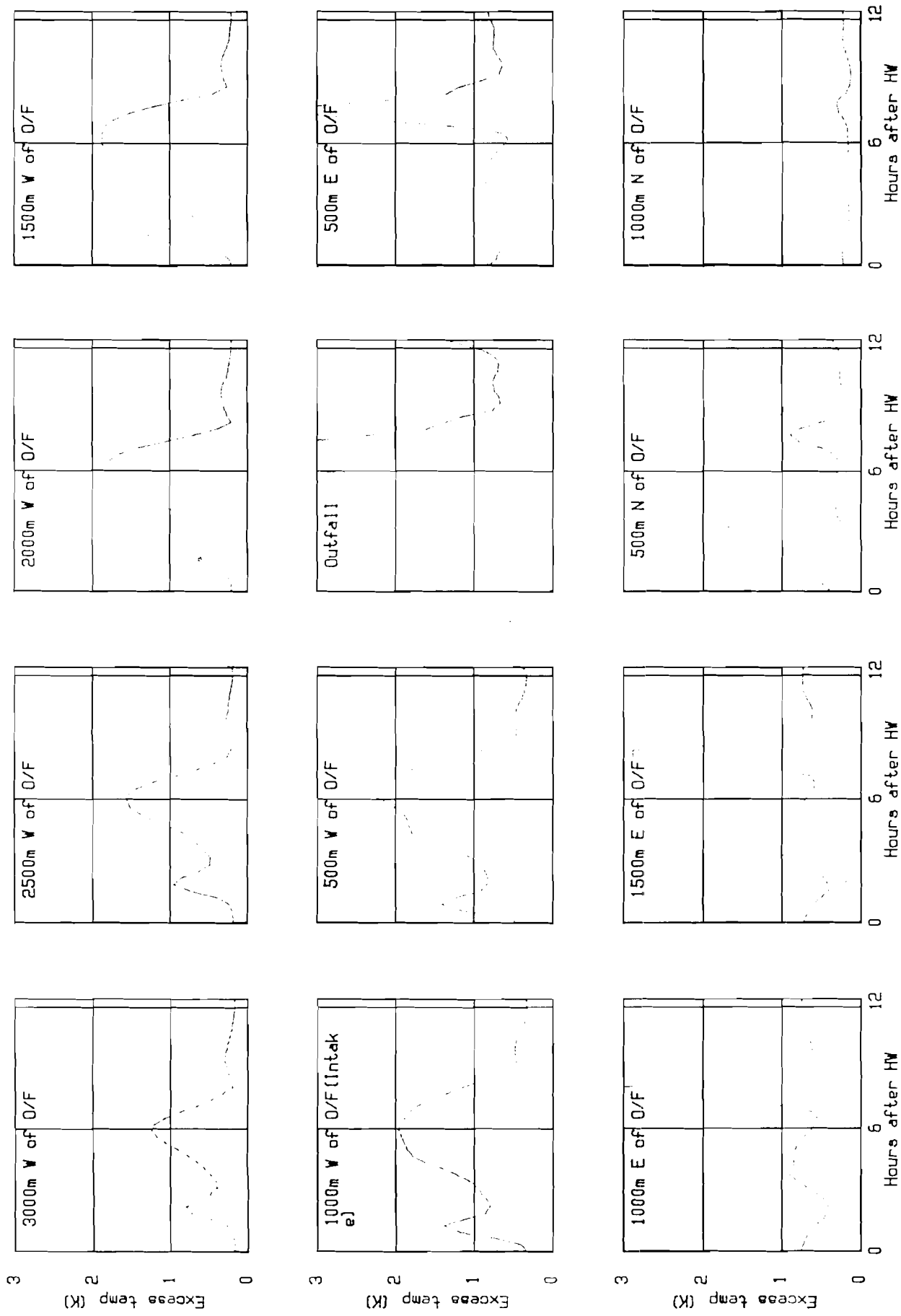


Fig 14 Far field model sensitivity
Heat input at outfall

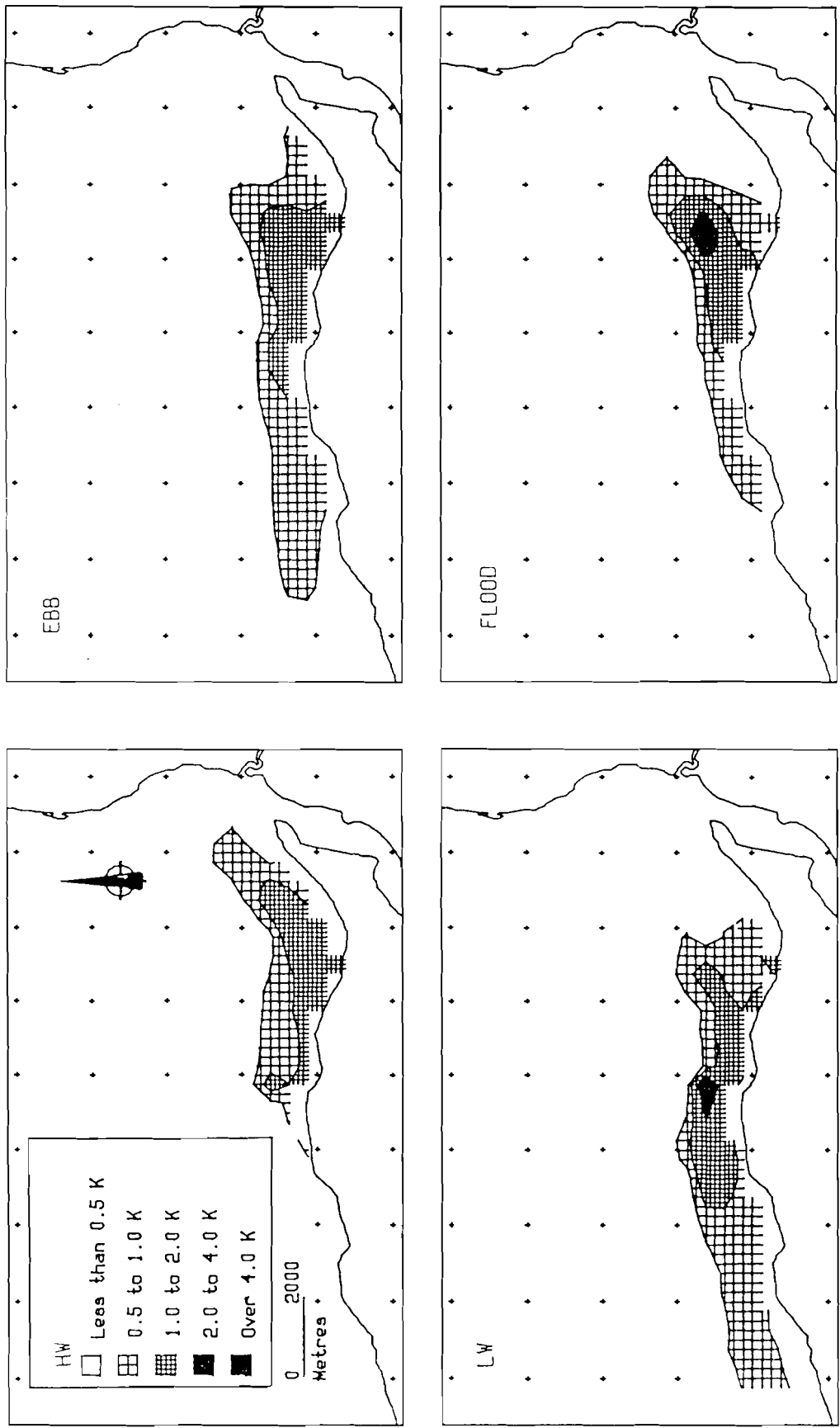


Fig 15 Far field model sensitivity
Heat input at outfall

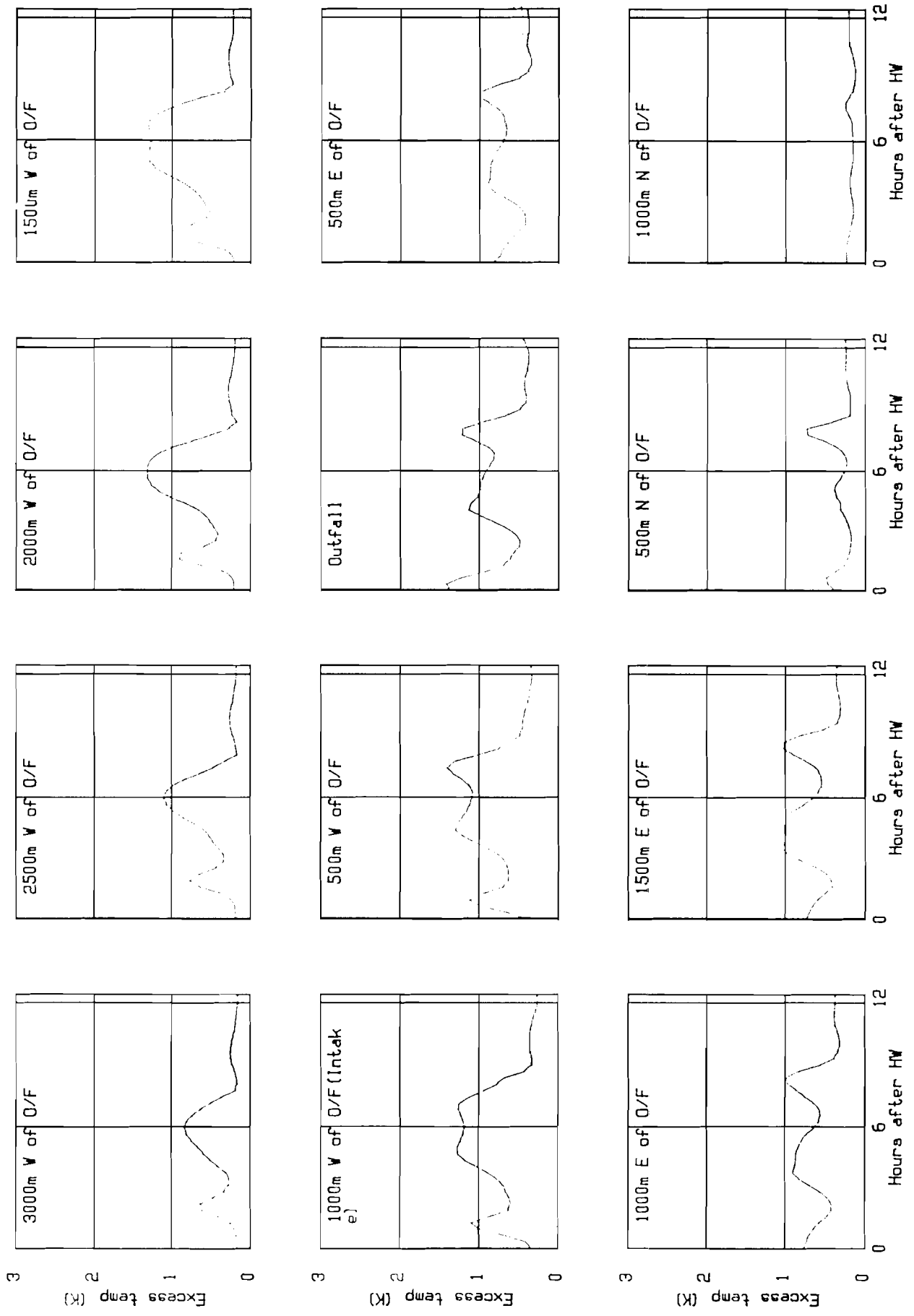


Fig 16 Far field model sensitivity
No heat input on last tide

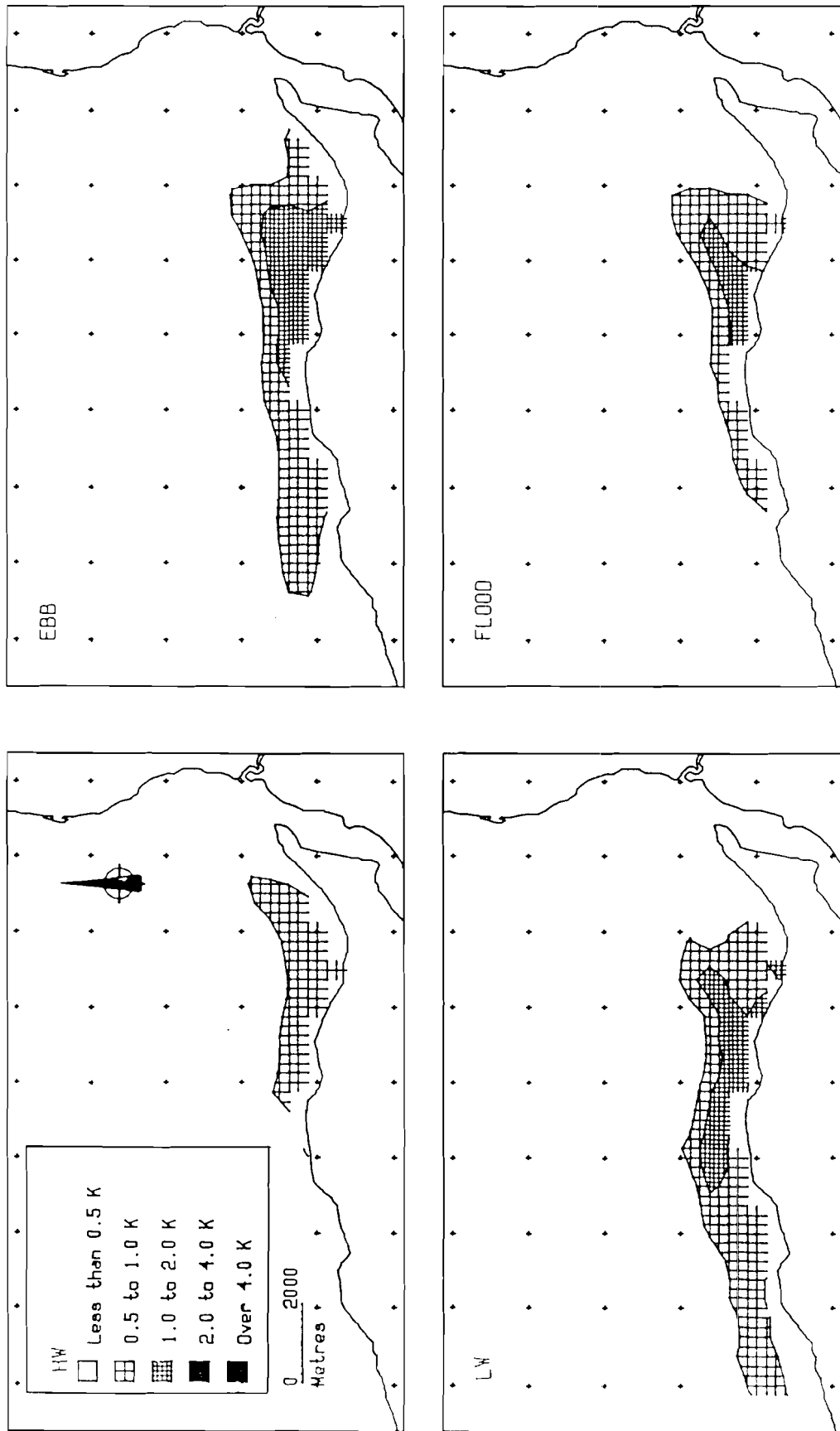


Fig 17 Far field model sensitivity
No heat input on last tide

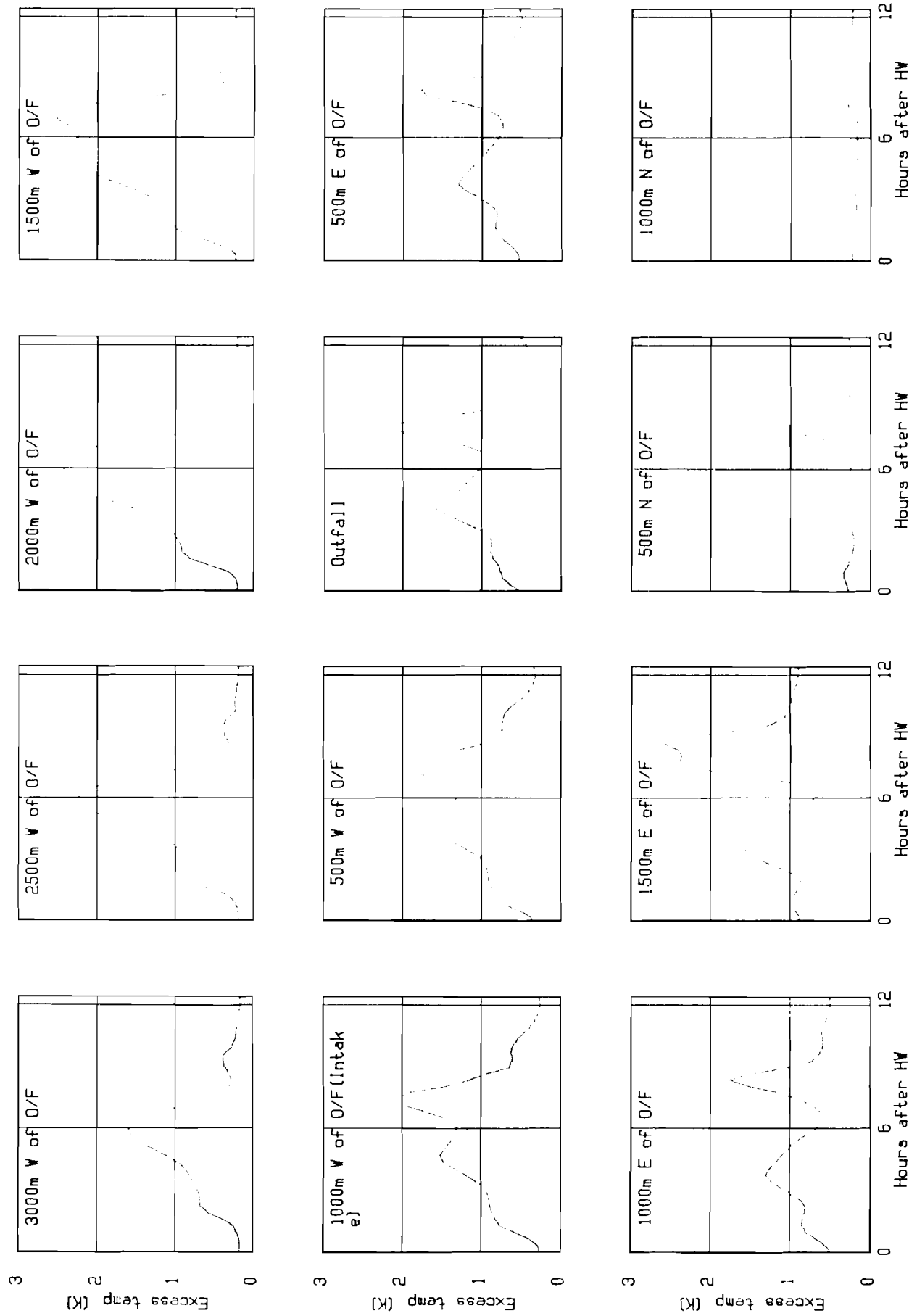


Fig 18 Far field model sensitivity
Heat input at A & B

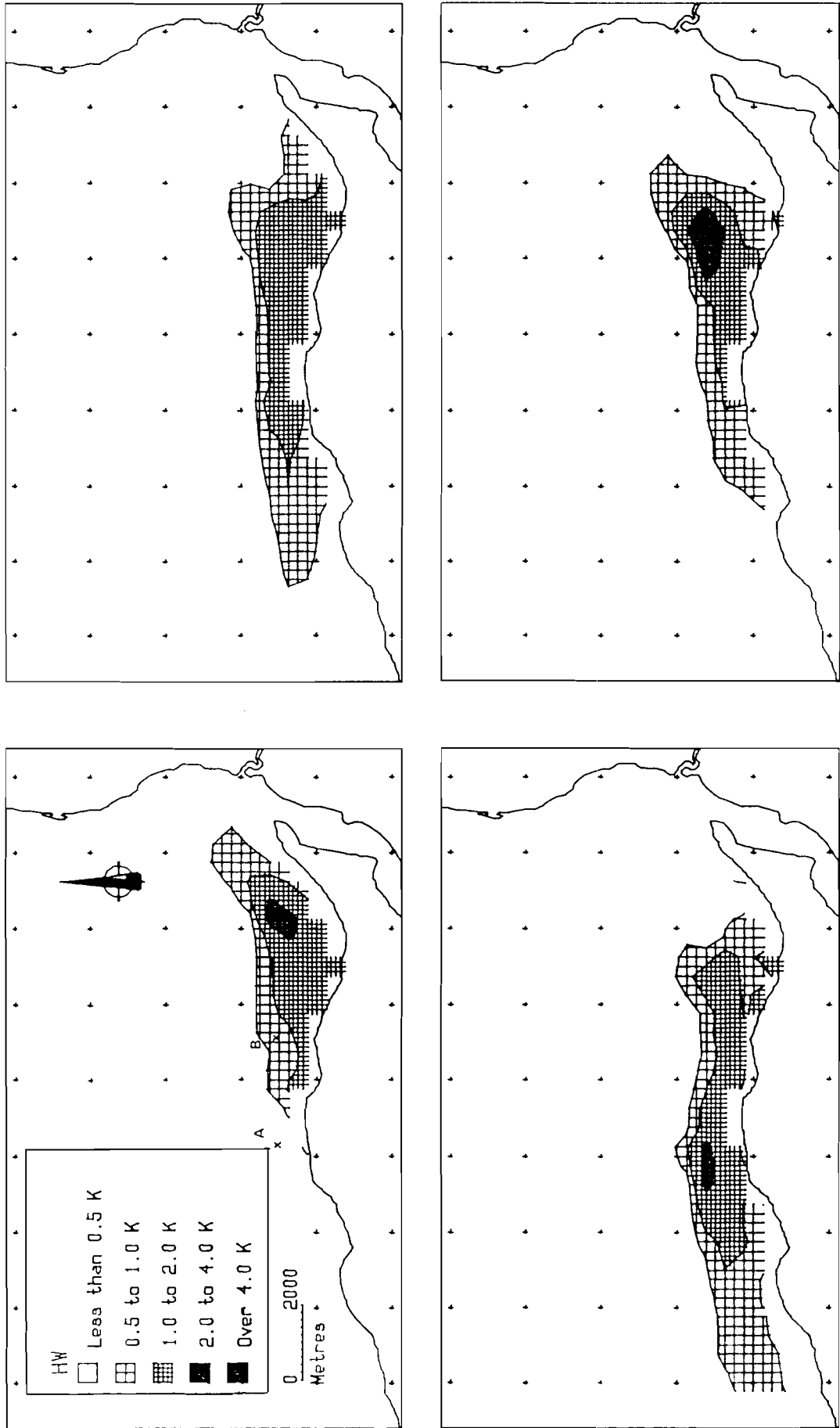


Fig 19 Far field model sensitivity
Heat input at A & B

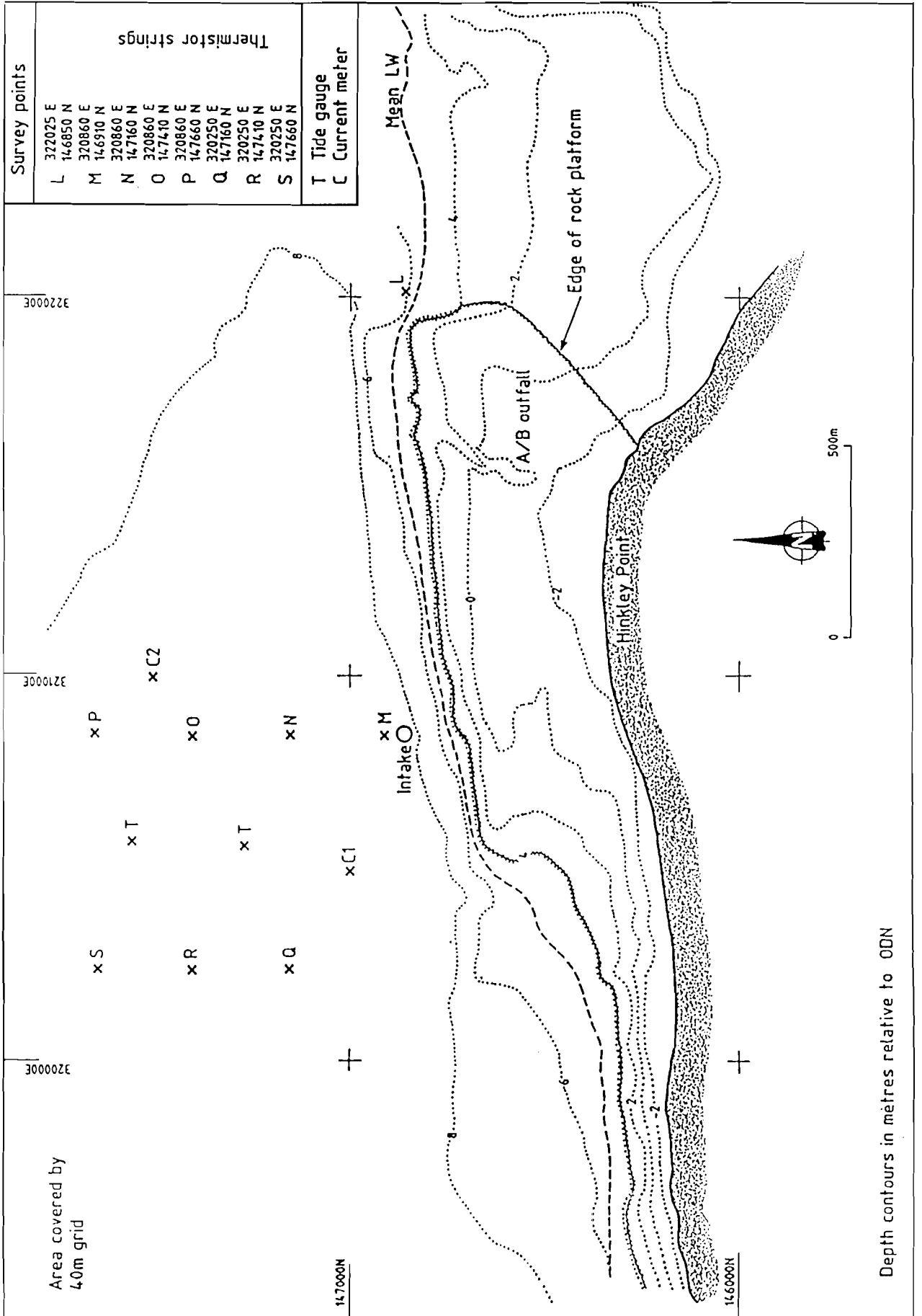


Fig 20 Hinkley survey positions

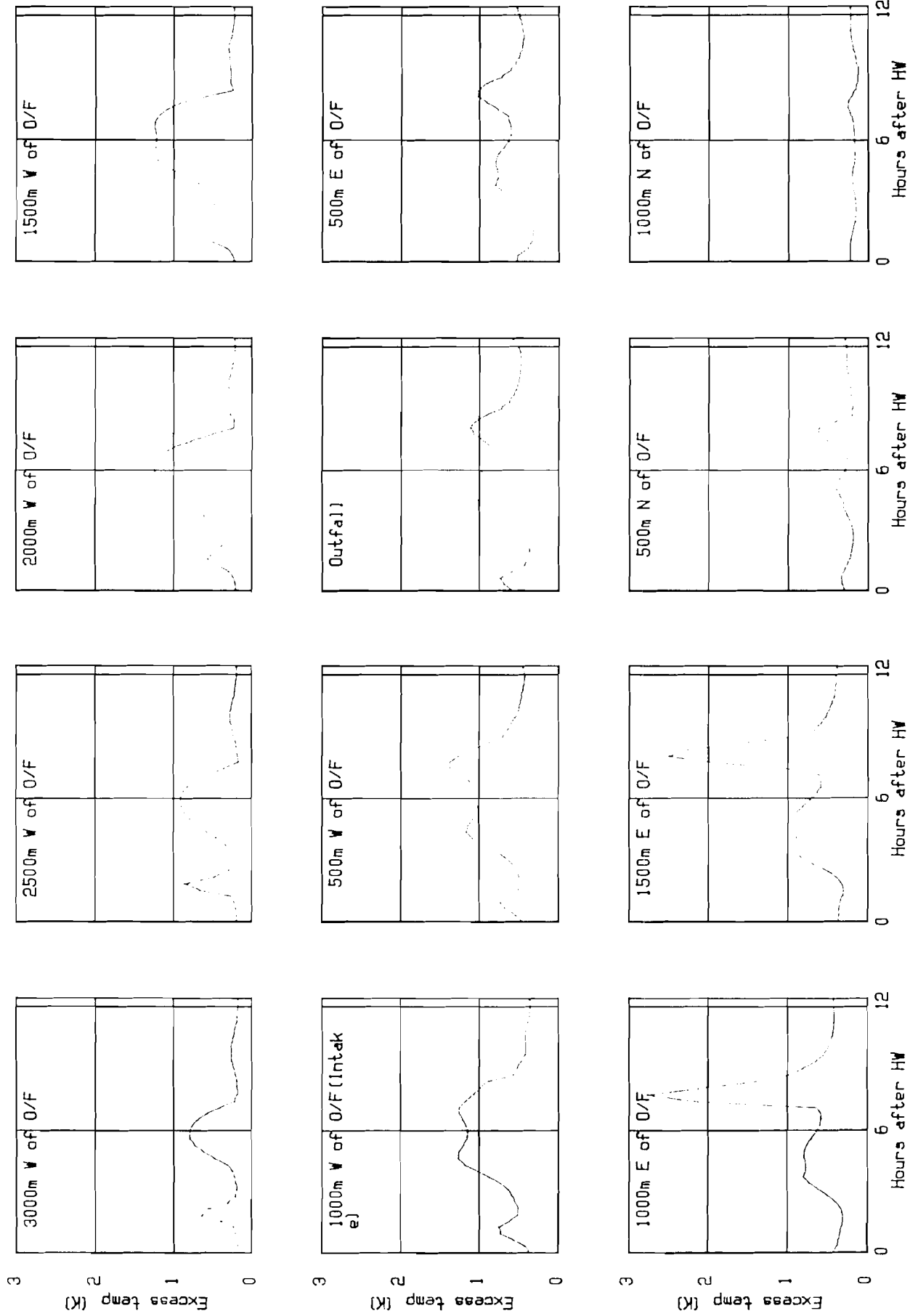


Fig 21 True far field temperature histories

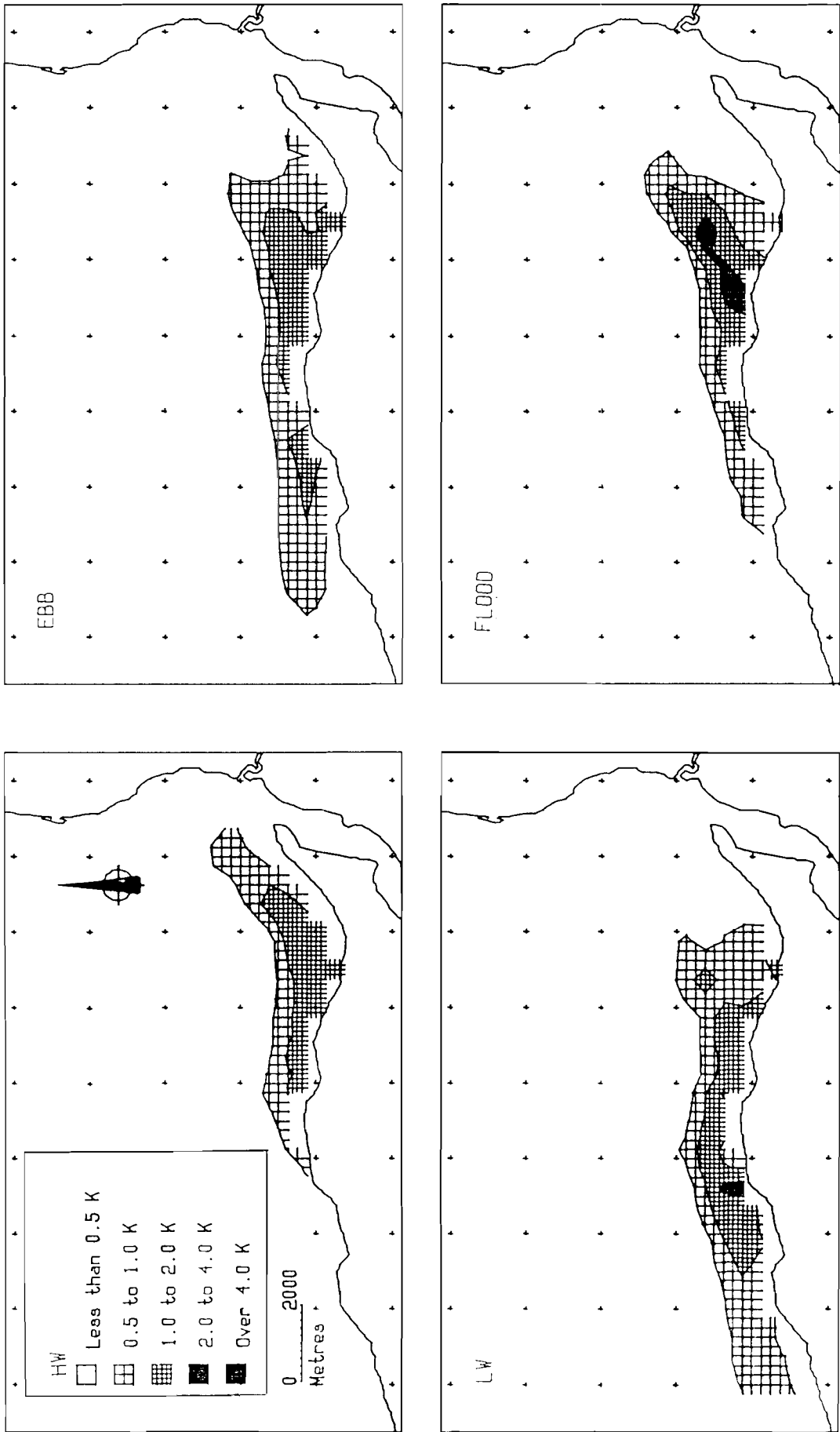


Fig 22 True far field temperature contours

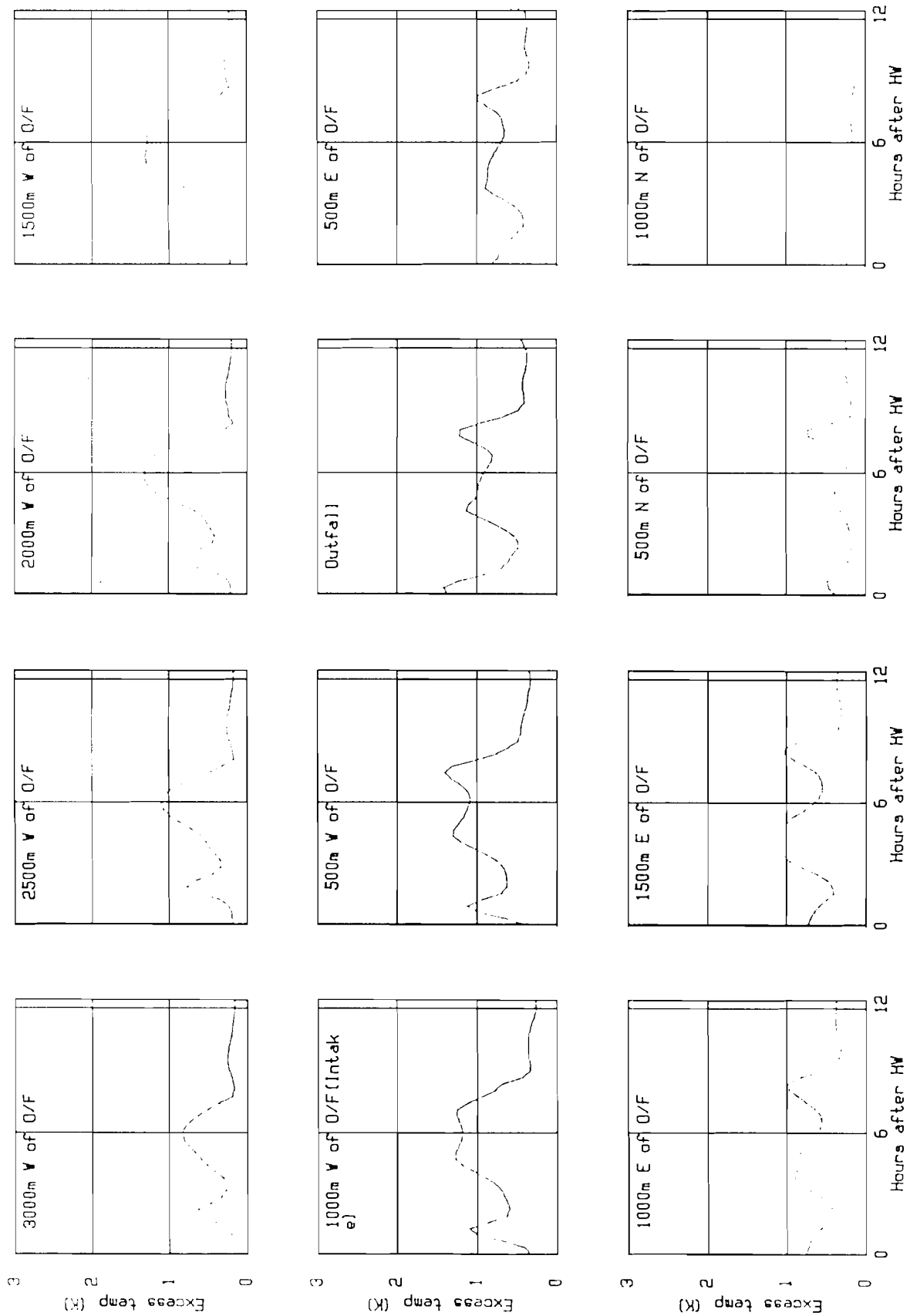


Fig 23 Far field temperatures
no primary heat

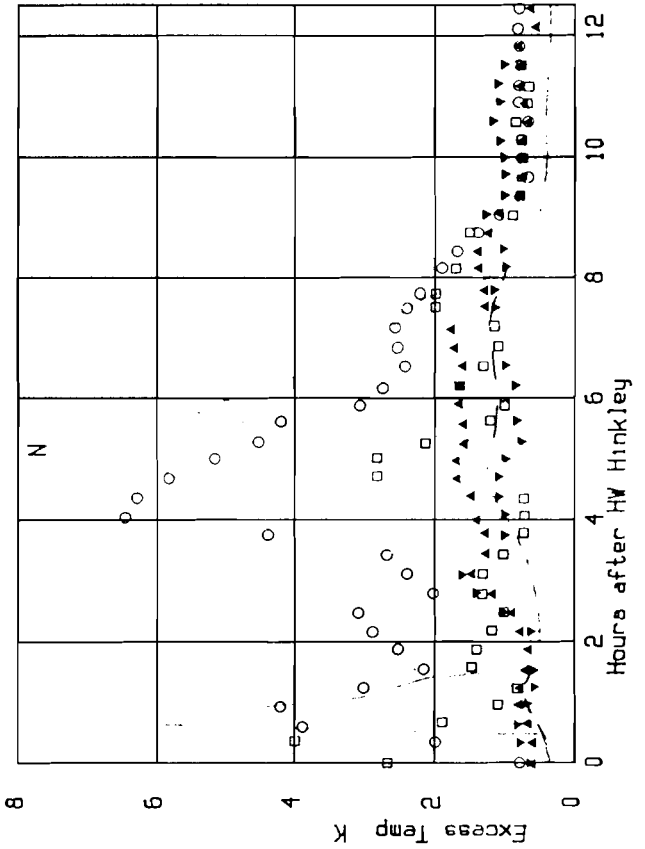
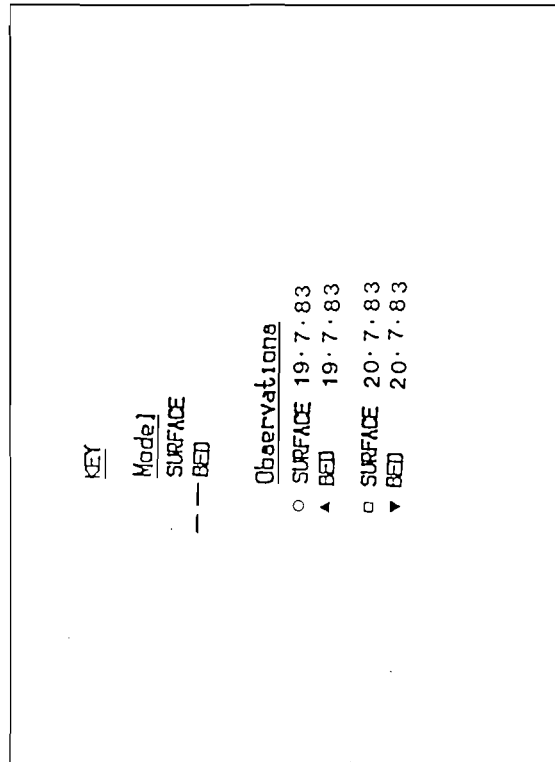
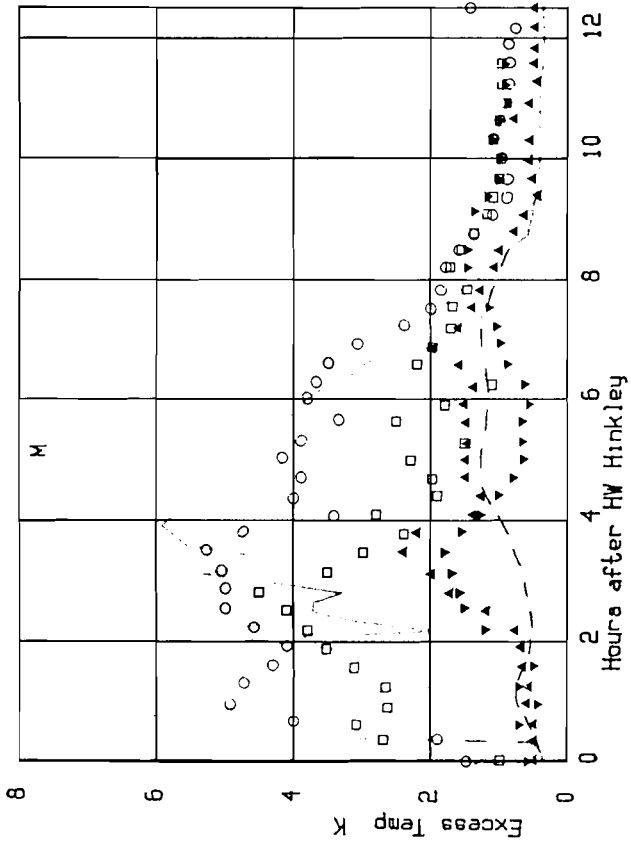


Fig 24 Total heat field comparison with data